



UNIVERSITÀ DEGLI STUDI DI PADOVA

Department of Comparative Biomedicine and Food Science

School of Agricultural Sciences and Veterinary Medicine

Second Cycle Degree (MSc) in

Biotechnologies for Food Science

Role of Calcium-Dependent Kinases in Arabidopsis Root Hair Responses to Mechanical Forces

Supervisor:

Prof. Jian Xu

Co-supervisor:

Prof. Alessandro Bertoli

Submitted by:

Abolfazl Yousefzadeh

Shourbolagh

Student Id: 2088694

Academic year 2024/2025

Acknowledgment

This project wouldn't have been possible without some truly wonderful people and institutions, and I'm so grateful for their support. First of all, a huge thank you to my supervisor at Radboud University, Professor Jian Xu, Chair of Plant Systems Physiology. From the very beginning, he not only gave me the incredible chance to pursue this project under his guidance, but also offered invaluable advice every step of the way. What truly made a difference was his belief in me and the freedom he gave me to shape my own research. That trust was incredibly empowering. I'd also like to express my sincere appreciation to Radboud University itself, and especially the Department of Plant and Animal Biology. They provided such a fantastic environment and all the resources I needed. And to all the colleagues I had the pleasure of working with – thank you for the camaraderie and for making my time here so enriching. Finally, my heartfelt thanks go to my home supervisor, Professor Alessandro Bertoli, who was a constant source of help and guidance throughout my thesis journey. And of course, to my home university, the University of Padova, for giving me this amazing opportunity to study at such a top-ranking institution.

Abstract

Plants increasingly struggle with mechanical stress in compacted soils, a growing problem amplified by climate change. Although we know root hairs are essential for absorbing water and nutrients, the exact molecular mechanisms enabling them to sense soil pressure have remained mostly unclear. In my master's research, I aimed to discover how specific calcium-dependent protein kinases (CPKs) namely CPK4 and CPK11 and the protein ANNEXIN1 influence the responses of *Arabidopsis thaliana* root hairs to mechanical stress.

To accurately study these delicate cellular processes, I developed two highly specific root-hair isolation methods: Cryo-Mechanical Disruption and freeze-thaw lysis, that consistently achieved over 90% hair RNA purity. Using knockout mutants (*cpk4*, *cpk11*, *annexin1*) and agar gradients simulating soil compaction (0.5%, 0.8%, 1%, 1.25%, 1.5% Agar Concentration), I found distinct responses: *cpk4* hairs showed early stress sensitivity but adapted at higher pressures; *cpk11* initially outperformed wild-type but sharply declined under severe stress; ANNEXIN1 was critical, with knockout lines almost completely halting hair growth at high stress. qPCR analysis revealed compensatory gene expression between CPK4 and CPK11, and similar responses in rice highlighted evolutionary conservation. These findings enhance our understanding of root hair mechanosensory systems and provide valuable insights for developing stress-resilient crops.

Table of Content

Acknowledgment	1
Abstract	2
1. Introduction	8
1.1. Climate change.....	8
1.2. Types of Stress Affecting Plants.....	8
1.2.1. Biotic stress.....	8
1.2.2. Abiotic stresses.....	9
1.3. Mechanical stress.....	10
1.4. Soil Compaction.....	11
1.5. Root hair cells.....	12
1.5.1. Structure of root hair.....	13
1.6. Root Hair Functions.....	14
1.6.1. Water and Nutrient Uptake.....	14
1.7. Root Hair as a Model for Stress Studies.....	14
1.8. Arabidopsis thaliana as an ideal Model Organism.....	15
1.8.1. Model Organism with Extensive Genetic Resources.....	15
1.8.2. Short Life Cycle and Similarities to Crops.....	15
1.8.3. Conservation of Stress Pathways Enables Cross-Species Translation	16
1.9. Plant Mechanosensing.....	16
1.9.1. Signal Transduction Pathways.....	18
1.9.2. Reactive Oxygen Species (ROS).....	18
1.9.3. MAPK Signaling Pathway.....	18
1.9.4. Calcium Signaling.....	19
1.10. Calcium-Dependent Protein Kinase (CDPK/CPK) Family.....	21
1.10.1. Interaction in Stress Signaling.....	22
1.10.2. CDPK Subfamilies, Members, and Stress Roles.....	24
1.10.3. Candidate genes for Mechanical Stress Regulation in Root Hairs..	25
2. Aim of the Study	25
3. Material and Methods	26
3.1. Development of Root Hair Isolation Methods.....	26
3.1.1. Cryo-mechanical disruption.....	26
3.1.2. The freeze-thaw lysis.....	27
3.1.3 Validation of Root Hair Isolation.....	27

3.1.4. Microscopic Validation.....	28
3.1.5. Gel-Based RNA Quality Assessment.....	29
3.1.6. Molecular Marker Validation.....	29
3.2. In Silico Analysis of Mechanosensitive Genes and Stress Responses.....	30
3.3. Root Cell-Type Specific Expression Analysis via RootCellAtlas.....	30
3.4. RNA-seq Analysis of Compacted Soil Stress in Rice Roots.....	31
3.4.1. Differential Gene Expression and Filtering.....	31
3.4.2. GO Annotation and Arabidopsis Homologs.....	31
3.5. QTL Mapping of Mechanosensory Candidates Using AraQTL.....	32
3.6. Plant Material and Experimental Conditions.....	32
3.7. Root Hair Phenotyping.....	32
3.8. RT-PCR and RT-qPCR.....	34
4. Results.....	35
4.1. Development and Validation of Root Hair Isolation Methods.....	35
4.1.1. Method Efficiency and Visual Validation.....	35
4.1.2. RNA Yield and Quality.....	35
4.1.3. Marker-Based Validation of Hair Specificity.....	36
4.2. In Silico Analysis of Mechanosensitive Genes and Stress Responses.....	37
4.3. Root Hair Cell-Type Specific Expression (RootCellAtlas).....	39
4.4. Cross-Species Transcriptomic Analysis of Soil Compaction Response in Rice	43
4.4.1. Identification of Differentially Expressed Genes.....	43
4.5. QTL Mapping Suggests Co-Regulation of Mechanosensitive Genes.....	46
4.6. Confirmation of T-DNA Insertion Mutants.....	46
4.7. Root Hair Phenotyping Under Compacted Agar Conditions.....	47
4.7.1. Stress-Induced Changes in Root Hair Growth.....	48
4.7.2. Mutant Sensitivity Relative to Wild-Type.....	48
4.7.3. Root Hair Length Analysis (0.8% Stress).....	49
4.7.4. Root Hair Density Analysis.....	50
4.7.5. First Root Hair Emergence Pattern.....	50
4.8. RT-PCR and RT-qPCR.....	52
Conclusion.....	54
References.....	56

1. Introduction

1.1 Climate change

As global temperatures rise due to climate change, plants face increasing exposure to extreme environmental conditions that impose significant mechanical stress. Prolonged heat and drought lead to drier soils, which undergo densification and compaction, reducing soil porosity and creating tougher barriers for root and root hair penetration (Koevoets et al., 2016; Colombi et al., 2018). Concurrently, more frequent extreme precipitation events, such as heavy rainfall and snowfall, disrupt soil structure—inducing surface crusting, aggregate breakdown, and root damage through impact forces (Bowles AM et al., 2022). In combination, these climatic factors create a challenging mechanical environment for plant roots: compacted, crusted soil layers resist root elongation and root hair development, impairing water and nutrient uptake essential for plant growth (Zhu et al., 2024; MDPI study, 2023) .

1.2 Types of Stress Affecting Plants

Plants have undergone evolutionary changes over centuries in response to abiotic and biotic stresses, but human activities over the past 200 years have introduced novel stressors, including habitat transformation, reduced biodiversity, and ecosystem pollution (Vasseur et al., 2018). Both biotic and abiotic stressors are major limiting factors for plant growth and productivity, contributing to significant yield losses and biodiversity decline (Zandalinas et al., 2021).

1.2.1 Biotic stress

Biotic stress refers to the negative impact of living organisms such as bacteria, fungi, nematodes, and viruses on plant roots and root hairs (Dodds PN , 2010). These interactions often disrupt cellular integrity and function through the activation of immune signaling, hormonal modulation, and localized structural changes (Millet et al., 2010).

Biotic stress can alter root development by modifying phytohormone balances, including auxin, ethylene, and salicylic acid, as well as initiating reactive oxygen species (ROS)

production and defense-related gene expression (Dodds PN , 2010). Additionally, biotic stress can affect nutrient uptake efficiency and alter the spatial distribution of root hairs, which has downstream consequences for plant fitness and survival (Millet et al., 2020).

The perception of biotic stress is often mediated by pattern recognition receptors (PRRs) located on the plasma membrane of root cells, which detect microbe-associated molecular patterns (MAMPs) and trigger downstream signaling pathways (Hückelhoven & Panstruga, 2023).

Soil-borne bacteria such as *Pseudomonas oryzae* influence root system architecture through non-volatile signal molecules, enhancing lateral root density via ethylene-responsive transcription factors (e.g., ERF109) and reactive oxygen species (ROS)-dependent pathways involving glutathione and strigolactone signaling. Pathogenic *Agrobacterium tumefaciens* induces crown gall formation by transferring T-DNA-encoded auxin biosynthesis genes (*iaaM*, *iaaH*), elevating IAA and phenylacetic acid (PAA) levels in infected roots and disrupting normal root development (Chen et al., 2020).

1.2.2 Abiotic stresses

Plants growing under abiotic stress conditions—including drought, salinity, heat, and nutrient scarcity—exhibit wide-ranging structural, physiological, and molecular adaptations within both roots and root hairs (Koevoets et al., 2016; Salazar-Henao et al., 2016). Drought stress often triggers the formation of "drought-rhizogenesis" roots:

specialized, short, swollen, hairless lateral roots that preserve turgor during water deficit and rapidly regenerate hair-bearing zones upon rehydration (Koevoets et al., 2016).

Prolonged drought also reduces root hair density and length, limiting water uptake capacity, while heat stress further shortens hair lifespan through effects on membrane stability and reactive oxygen species (ROS) accumulation (Salazar-Henao et al., 2016).

Saline environments impose dual osmotic and ionic stress on roots, leading to inhibited elongation, altered architecture, and disturbed hormone signaling—particularly ABA and auxin pathways (Koevoets et al., 2016). Specifically, salt exposure downregulates root hair regulators (e.g., RHD6) via ABA-responsive transcription factors, leading to shorter and fewer hairs (Salazar-Henao et al., 2016). Root hairs also respond dynamically to nutrient limitations: phosphorus deficiency induces longer, denser root hairs mediated by RSL4 activation, whereas osmotic stress elicits GL2-dependent repression of hair growth, enhancing resource acquisition under challenging conditions (Koevoets et al., 2016).

Soil pH imbalance, whether acidic or alkaline, acts as a critical abiotic stressor that through

modulation of nutrient availability, ion toxicity, and hormone signaling (Kochian et al., 2015; Fendrych et al., 2018). Under acidic soil conditions ($\text{pH} \leq 5.5$), excess H^+ and Al^{3+} ions inhibit root elongation, reduce nutrient uptake, and trigger oxidative stress responses (Kochian et al., 2015).

Conversely, alkaline conditions ($\text{pH} \geq 8.0$) suppress root elongation and alter growth patterns such as waving and skewing, mediated by changes in auxin transporter localization (e.g., vacuolar trafficking of PIN7) and disruptions in acidification at the cell wall - an essential process for root hair emergence (Fendrych et al., 2018). High pH also inhibits root hair initiation and elongation by destabilizing cell wall relaxation mechanisms and altering Ca^{2+} and reactive oxygen species (ROS) oscillations critical for tip growth (Kochian et al., 2015; Fendrych et al., 2018).

Moreover, Abiotic chemical stress includes exposure to heavy metals, herbicides, and industrial pollutants, adversely affect plant development through cytotoxicity, hormone imbalance, and metabolic disruption (DalCorso et al., 2019; Riaz et al., 2021). Cadmium (Cd), for instance, disrupts primary root meristem activity by dysregulating auxin-cytokinin signaling, perturbing expression of key regulators such as SCR and PIN proteins (DalCorso et al., 2019). Cd also reduces root hair density and length in *Arabidopsis*, while higher hair abundance correlates with increased Cd translocation to shoots (Riaz et al., 2021).

1.3 Mechanical stress

Mechanical stress in plants, originating from physical impediments such as compacted soil, freezing-induced ice expansion, or insect herbivory, activates a complex interplay of signaling pathways that converge on common molecular cascades involving membrane mechanosensors, calcium influx, reactive oxygen species (ROS), and hormonal regulation. Upon mechanical deformation, such as that caused by soil particles or root compression, mechanosensitive ion channels, including Mid1-Complementing Activity 1 (MCA1) and Mechanosensitive Channel of Small Conductance-Like (MSLs), are activated, leading to rapid cytosolic Ca^{2+} spikes and transient apoplastic alkalization (Nakagawa et al., 2007; Hamilton et al., 2015). These events trigger the expression of mechanoresponsive genes, such as TCH1–TCH4, which modulate cytoskeletal dynamics and cell wall remodeling, thereby influencing root hair growth and directional responses (Xu et al., 1995).

Mechanical damage, such as that induced by freezing or insect feeding, similarly elicits Ca^{2+} influx, ROS production, and activation of mitogen-activated protein kinase

(MAPK) cascades, which stimulate jasmonic acid (JA) and ethylene signaling, resulting in localized growth arrest and defense activation (Pomiès et al., 2017).

Ethylene signaling specifically mediates growth cessation in response to mechanical impedance, such as barriers or root bending, through the EIN3–WDL5–microtubule axis, highlighting its role in cytoskeletal reorganization under both mechanical and freezing-induced stresses (Zheng et al., 2016). Thus, whether roots encounter biotic damage from insect herbivory, abiotic stress from cold-induced cell damage, or physical resistance from soil, the underlying mechanotransduction system—characterized by Ca²⁺ influx, ROS production, hormonal integration, and transcriptional reprogramming—demonstrates a unified response across diverse environmental challenges.

1.4 Soil Compaction

Anthropogenic climate change has intensified global surface temperatures, accelerating evaporation and exacerbating drought events, which lead to soil consolidation, reduced pore space, and increased bulk density, resulting in mechanical compaction without external physical pressure (Bengough et al., 2011). However, compaction is also directly caused by human activities such as heavy machinery, livestock (cattle), and even foot traffic, which exacerbate soil degradation independently of climatic factors (Ogorek et al., 2024). This process is amplified by repeated wet–dry and freeze–thaw cycles, which degrade soil structure and stability (Nawaz et al., 2013). Compacted and drier soils increase mechanical impedance, restricting root penetration, elongation, volume, and surface area, particularly limiting access to water, oxygen, and immobile nutrients like phosphorus and nitrogen, which depend on diffusive processes (Tracy et al., 2011). Mechanical impedance becomes a primary growth-limiting factor when soil penetration resistance exceeds ~2 MPa in crops like maize and peanut (Bengough et al., 2011).

The downstream consequences of restricted root development are severe: diminished water and nutrient uptake reduces plant productivity and resilience to abiotic stressors, with crop yield reductions varying from modest to catastrophic depending on soil texture, crop species, and climate severity, where topsoil compaction often proves more detrimental than subsoil compaction (Bengough et al., 2011). Persistently compacted soils alter cropping patterns, compromise agricultural sustainability, promote erosion, suppress microbial biodiversity, and disrupt ecosystem services such as carbon sequestration (Nawaz et al., 2013). Soil compaction significantly impacts root system architecture and root hair development by

increasing bulk density, reducing porosity, and mechanically impeding root penetration. Increased gas diffusion resistance in compacted soils leads to ethylene accumulation near root tips, activating growth-inhibitory pathways in *Arabidopsis thaliana*; ethylene-insensitive mutants maintain root growth in compacted layers, suggesting ethylene, rather than mechanical force, drives early growth suppression (Jacobsen et al., 2021). Additionally, reactive oxygen species (ROS), auxin, and ethylene form an interconnected signaling network modulating cell elongation and radial expansion in response to physical barriers, adjusting root growth to compaction stress (Jacobsen et al., 2021). At the root hair level, compaction reduces hair length and density through disrupted cytoskeletal dynamics and impaired cellular turgor in trichoblasts, though some genotypes exhibit compensatory increases in hair growth (Bengough et al., 2011).

Root hairs also influence rhizosheath formation, reducing soil hardness and elasticity at the root–soil interface, as evidenced by X-ray computed tomography (CT) imaging under field conditions (Helliwell et al., 2017). In crops like maize and rice, compaction induces root modifications, including increased cortical thickness, reduced branching, and regulated auxin-dependent root hair elongation, with enhanced expression of genes like *OsYUC8* promoting hair length and improving anchorage in dense soils (Huang et al., 2022).

1.5 Root hair cells

Root hairs are single-celled tubular extensions originating from specialized epidermal cells known as trichoblasts within the root's maturation zone. They differentiate from the root apical meristem, emerging just beyond the elongation zone, and typically have a lifespan of 1–3 weeks before being shed. These structures significantly enhance plant function and productivity by dramatically increasing the root surface area, thereby facilitating efficient uptake of water and immobile nutrients such as phosphorus and potassium. In spring wheat cultivated under low-fertility soil conditions, long and dense root hairs have been shown to significantly contribute to the early uptake of micronutrients, although vigorous whole-root growth also plays a critical role. In agricultural contexts, root hair traits—such as density, length, and plasticity—are valuable targets for crop improvement, as they enhance resource-use efficiency and yield stability in nutrient-poor, drought-prone, or compacted soils. The relatively simple genetic control of root hair traits makes them ideal candidates for breeding programs and functional studies. Furthermore, their accessibility and reproducibility position root hairs as significant models in cell biological research, particularly for

investigating tip growth, signal transduction, and plant–environment interactions (Gahoonia and Nielsen, 2004).

1.5.1 Structure of root hair

Root hairs are tip-growing, tubular extensions of single trichoblast epidermal cells in the root maturation zone, uniquely adapted for absorption and environmental interaction. At the ultrastructural level, root hairs exhibit pronounced cytoplasmic polarity, with an apical zone enriched in vesicles, Golgi, endoplasmic reticulum, and organized actin filaments, indicative of active growth, while the subapical shank contains vacuoles and accumulated organelles (Miller et al., 1999). Their cell walls are specialized, comprising a flexible primary wall at the tip with short, randomly oriented cellulose microfibrils embedded in a pectin and hemicellulose matrix to enable expansion, and a more rigid subapical layer with helically arranged microfibrils for mechanical stability (Park et al., 2011). Cellulose synthase–like proteins, such as CSLD2 and CSLD3, localize to the growing tip and are critical for cellulose-like microfibril polymerization during tip growth, while xyloglucan, pectin, and expansins (EXPA7, EXPA18) regulate wall loosening and extensibility essential for elongation (Park et al., 2011; Vissenberg et al., 2001). Cell wall thickness typically ranges from ~100–200 nm at the tip to ~300–500 nm along the shank, with microfibril diameters of approximately 3–4 nm, consistent with single synthase outputs (Park et al., 2011). Internally, the actin cytoskeleton forms thick longitudinal bundles in the shank and a fine actin mesh at the apex, guiding vesicle trafficking in conjunction with motor proteins such as myosin XI to deliver cell wall materials, while microtubules maintain polarity and directional growth (Miller et al., 1997; Baluška et al., 2000). Cell shape and turgor maintenance are tightly regulated through vacuole dynamics, ion transport, and osmotic balance, supporting rapid volumetric expansion (~50 fL min⁻¹) during tip growth (Baluška et al., 2000).

1.6 Root Hair Functions

1.6.1 Water and Nutrient Uptake

Root hairs, characterized by their precise shape, length (0.5–1.7 mm), density (17–21 mm⁻²), and occasional branching, significantly enhance the absorptive surface area of roots while

exhibiting greater resistance to mechanical stress, such as soil compaction, compared to thicker roots. In wheat, longer root hairs are positively correlated with increased biomass, grain count per spike, and relative water content under both normal and water-limited conditions, serving as critical indicators of yield potential. Field studies in barley and maize demonstrate that root hairs improve phosphorus and potassium uptake, resulting in a 15–30% yield increase, particularly under nutrient- and water-stressed conditions, with hairless maize mutants exhibiting significantly lower yields compared to hair-bearing genotypes. Additionally, root hairs contribute to soil adhesion and rhizosheath formation, enhancing soil structure and moisture retention, which is particularly vital in marginal soils. These conserved functions of root hairs across diverse crop species underscore their critical role in enhancing plant resilience and productivity.

Consequently, root hair traits are increasingly recognized as valuable breeding targets for improving drought tolerance, nutrient efficiency, and yield stability in modern agriculture (Marin et al., 2021).

1.7 Root Hair as a Model for Stress Studies

Root hairs serve as highly sensitive, independent, and early-responding sensors to environmental and mechanical stress, making them ideal candidates for studying root stress responses. Their growth is exquisitely sensitive to external conditions, with even subtle variations in medium stiffness, nutrient composition, or moisture content eliciting measurable changes in growth rate, tip dynamics, and nuclear positioning, such as reduced tip and nuclear velocities in increasingly stiff agar (Le Gall et al., 2024). Additionally, root hairs exhibit a predictable, apical tip-growth pattern with defined elongation rates and lifespans, enabling reliable comparative analyses across treatments and genotypes (Le Gall et al., 2024). A critical advantage is the independent behavior of each root hair, even on the same root; when some hairs encounter localized physical obstacles, such as rocks or compacted soil regions, their growth is impeded, while neighboring hairs continue unaffected, allowing for internal controls within the same root and minimizing confounding systemic effects (Le Gall et al., 2024). Furthermore, root hairs are among the first structures to engage with soil, acting as front-line responders to environmental changes. Their immediate responses to mechanical impedance, moisture variation, and nutrient heterogeneity provide rapid insights into root–soil interaction dynamics (Kohli et al., 2022). Root hairs also demonstrate significant phenotypic plasticity, modulating length, density, and

branching in response to abiotic stresses like nutrient deficiency or salinity, often mediated by hormonal signaling involving auxin, ethylene, and abscisic acid (ABA) (Kohli et al., 2022) (Figure 1.B).

1.8 Arabidopsis thaliana as an ideal Model Organism

1.8.1 Model Organism with Extensive Genetic Resources

Arabidopsis thaliana is a cornerstone model organism in plant biology, owing to its compact, fully sequenced genome (~135 Mb) and extensive genetic and molecular resources (Provart et al., 2016). The Arabidopsis Information Resource (TAIR) database provides access to a vast array of T-DNA insertion lines, EMS mutants, RNAi lines, and CRISPR-Cas9 edited lines, enabling precise functional genomics studies (Berardini et al., 2015). These tools have facilitated the identification and manipulation of genes critical for mechanosensing, including mechanosensitive ion channels (MSL, MCA), receptor-like kinases (FER, THE1), and transcriptional regulators (WDL5, TREP1), which are pivotal in mechanical stress signaling (Provart et al., 2016; Bacete et al., 2018). Furthermore, the simplicity of transformation via the floral dip method allows for efficient generation of transgenic lines for stress assays and reporter analyses, enhancing the study of mechanosensory responses (Bacete et al., 2018).

1.8.2 Short Life Cycle and Similarities to Crops

The rapid lifecycle of *Arabidopsis*, completing seed-to-seed development in approximately six weeks, makes it highly amenable to laboratory conditions (Provart et al., 2016). This short generation time enables rapid assessment of genetic modifications across generations, a critical feature for long-term mechanical stress experiments and mutant screening. Its small size and ability to grow on agar plates independent of soil facilitate controlled experiments involving mechanical stimuli, such as simulated soil compaction, touch, or osmotic stress (Bacete et al., 2018). Additionally, the small, transparent roots of *Arabidopsis* are particularly suited for live imaging techniques, such as confocal or spinning disk microscopy, which are essential for studying mechanical deformation, root hair dynamics, and intracellular signaling events, including calcium fluxes and cytoskeletal rearrangements (Provart et al., 2016) (Figure 1.A).

1.8.4 Conservation of Stress Pathways Enables Cross-Species Translation

Despite its simple dicot structure, *Arabidopsis* shares conserved stress response pathways with agronomically important crops, including those mediating mechanical stress responses. Components of calcium signaling, MAPK cascades, ROS signaling, and hormone responses activated by mechanical stress are highly conserved across dicots and monocots, such as rice (*Oryza sativa*), maize (*Zea mays*), and wheat (*Triticum aestivum*) (Jacobsen et al., 2021). Transcriptomic analyses have demonstrated that mechanical stimulation upregulates hundreds of conserved stress-related genes, including TCH4, CML, WRKYs, and XTHs, in both *Arabidopsis* and crop species, underscoring the evolutionary conservation of mechanosensory machinery and its relevance for translational research (Jacobsen et al., 2021).

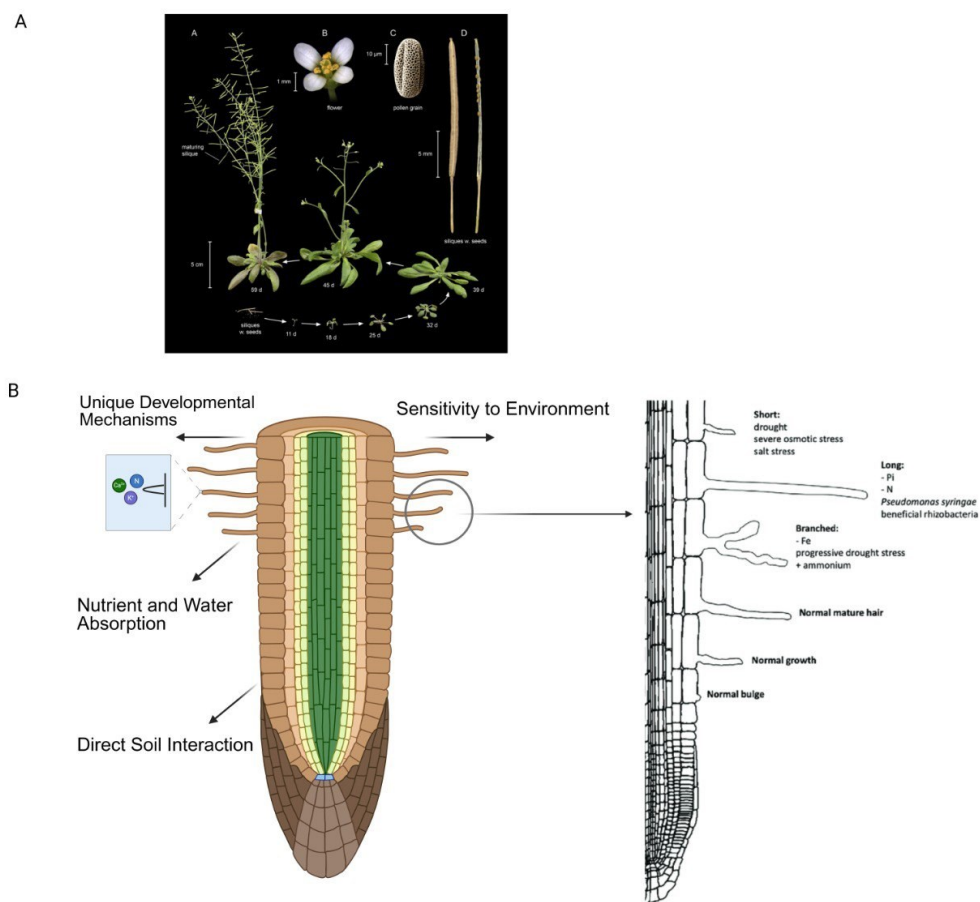


Figure 1. Journey Through the Life of *Arabidopsis thaliana*. (a) This panel showcases the life stages of *Arabidopsis thaliana* from the Columbia (Col) accession, beginning with a seed (bottom left), progressing through a seedling at 11 days, a vegetative phase at 39 days, and reaching reproductive maturity at 45 days. Accompanying images include (b) a delicate flower, (c) a pollen grain captured via scanning electron microscopy, and (d) mature siliques (seed pods) at enhanced magnification (left: closed; right: open, revealing a few lingering seeds), (Provart et al., 2015), (A). Influence of Environmental Factors on

Arabidopsis Root Hair Growth. This diagram offers a detailed, longitudinal view of an Arabidopsis root, illustrating the development of root hairs under typical environmental conditions, providing a clear snapshot of their growth patterns in a natural setting(B) (Salazar-Henao et al., 2020).

1.9 Plant Mechanosensing

Plants perceive and respond to mechanical stimuli through an integrated mechanosensing network comprising mechanosensitive ion channels, receptor-like kinases, the cell wall–plasma membrane–cytoskeleton continuum, calcium influx, and hormonal signaling pathways. Mechanosensitive (MS) ion channels, including MscS-like (MSL), MCA, OSCA, Piezo-like, and TPK families, directly detect plasma membrane tension. Upon mechanical stress from stimuli such as touch, wind, or soil compaction, these channels open within milliseconds, mediating rapid Ca^{2+} and other ion fluxes as early events in mechanotransduction (Hamilton et al., 2015). For instance, Arabidopsis MCA1 and MCA2 are essential for efficient root penetration in hardened media, underscoring their role in root mechanics (Hamilton et al., 2015). Under soil compaction, root system architecture (RSA) undergoes distinct alterations: primary root growth is suppressed (e.g., 30% reduction in rice due to inhibited epidermal cell elongation), branching is reduced, and roots thicken via radial expansion of cortical cells, while crown root numbers may increase—though the adaptive value of thicker roots remains debated(Ogorek et al., 2024) Receptor-like kinases (RLKs), such as FERONIA (FER) and THESEUS1 (THE1), sense alterations in cell wall integrity. FER interacts with demethylesterified pectin, initiating ROP6 GTPase signaling and cytoskeletal reorganization under mechanical stress, while THE1 detects cell wall damage linked to cellulose biosynthesis defects, triggering downstream stress responses (Bacete et al., 2018). The cell wall–plasma membrane–cytoskeleton continuum serves as a physical and functional bridge for force transmission, with Hechtian strands and ER–PM contact sites, marked by proteins like SYT1 and VAP27, anchoring the cytoskeleton and mechanosensitive components to facilitate signal integration and structural adaptation (Bacete et al., 2018). The cytoskeleton, comprising actin and microtubules, reorganizes in response to mechanical stress to adjust cell morphogenesis, supporting load-bearing capacity and guiding directional growth (Hamilton et al., 2015). Hormonal pathways, particularly involving jasmonic acid, ethylene, auxin, and abscisic acid, mediate longer-term growth and developmental adaptations. Mechanostimulation induces jasmonic acid synthesis via MYC transcription factors, leading to cell wall reinforcement, defense priming, and structural modifications characteristic of thigmomorphogenesis (Chehab et al., 2012).

1.9.1 Signal Transduction Pathways

Following the detection of mechanical stress through mechanosensitive ion channels, receptor-like kinases, and cytoskeletal rearrangements, plants initiate a rapid calcium influx and reactive oxygen species (ROS) production, forming a primary signaling wave (Kohli et al., 2022). This early signal activates mitogen-activated protein kinase (MAPK) cascades, often via oxidative stress-sensitive kinases such as ANPs, MEKK1, MKK1/2, and MPK3/6, which phosphorylate downstream transcription factors to orchestrate stress responses (Kohli et al., 2022).

1.9.2 Reactive Oxygen Species (ROS)

Mechanical stress, including compression, bending, pressure, or root tip impingement, triggers a rapid, spatially localized burst of ROS in plant roots and root hairs, primarily mediated by NADPH oxidases (RBOHs) that generate superoxide (O_2^-), rapidly converted to hydrogen peroxide (H_2O_2) (Jacobsen et al., 2021). Simultaneously, ROS-sensitive Ca^{2+} channels open, amplifying calcium influx and establishing a positive-feedback loop (Jacobsen et al., 2021). At the molecular level, mechanical sensations detected by ion channels and cell wall-membrane disturbances activate RBOH proteins, driving localized ROS production. H_2O_2 diffuses through aquaporins, functioning as a second messenger that oxidizes thiol groups on key proteins and activates MAPK (e.g., MPK3/6) and calcium-dependent protein kinases (CDPKs), which phosphorylate effector proteins involved in gene expression, cytoskeletal rearrangement, ion flux regulation, and cell wall reinforcement (Kohli et al., 2022). ROS waves propagate intercellularly via plasmodesmata or apoplastic diffusion, coordinating mechanical stress signaling across root tissues (Fichman & Mittler, 2020). To prevent oxidative damage, antioxidant enzymes such as superoxide dismutase, catalase, and peroxidases are upregulated to maintain ROS homeostasis (Fichman & Mittler, 2020).

1.9.2 MAPK Signaling Pathway

In response to mechanical stress, such as root compression, bending, or soil impedance, plants activate specific MAPK cascades to transduce physical signals into adaptive biochemical responses. Mechanosensitive ion fluxes and ROS production activate MAP

kinase kinase kinase (MAPKKK) proteins like MEKK1 or ANP1, which phosphorylate MAP kinase kinases (MKKs, e.g., MKK2), subsequently activating MAP kinases MPK3 and MPK6 via dual phosphorylation of their TXY motifs (Kohli et al., 2022). Activated MPK3/6 phosphorylate diverse targets, including transcription factors (e.g., WRKYs, ERFs), the ethylene biosynthetic enzyme ACS, and ion transporters. MPK-mediated phosphorylation of ACS enhances ethylene synthesis, while WRKY phosphorylation upregulates stress-responsive genes, bolstering structural integrity and defense capacity (Jacobsen et al., 2021). Additionally, MPK3/6 can degrade cytokinin response regulators (e.g., ARR1/10/12), shifting hormonal balance toward growth suppression under mechanical impedance (Kohli et al., 2022). Loss-of-function mutants in MPK3/6 or upstream kinases (e.g., *mkk2*, *mekk1*) exhibit impaired touch-induced gene expression and reduced stress acclimation, underscoring the critical role of MAPK signaling in mechanotransduction (Jacobsen et al., 2021).

1.9.3 Calcium Signaling

Calcium signaling in plants involves transient and tightly regulated increases in cytosolic Ca^{2+} concentration ($[\text{Ca}^{2+}]_{\text{cyt}}$), functioning as a universal secondary messenger that translates diverse external cues into biochemical and physiological responses (figure 2) (Kudla et al., 2018). Calcium ions (Ca^{2+}) are indispensable for the plant life cycle, acting as both a vital mineral nutrient and versatile intracellular signaling molecule that plays crucial roles in plant growth, development, and stress responses (Zartdinova and Nikitin, 2023; Luan and Wang, 2021). In resting cells, $[\text{Ca}^{2+}]_{\text{cyt}}$ is maintained at approximately 100 nM, while extracellular and organellar calcium levels range from micromolar to millimolar, establishing a steep gradient that enables rapid influx upon channel activation (Kudla et al., 2018). When specific signals or stress factors are encountered, this pathway stimulates open calcium channels, causing an influx of calcium from the extracellular space into the cell cytosol (Kang et al., 2024). This signaling is triggered by various stimuli, including abiotic stresses (e.g., drought, salinity, extreme temperatures), biotic challenges (e.g., pathogens, herbivores), developmental cues, and mechanical stimuli such as touch, soil compaction, or wounding (Tian et al., 2020). The influx of calcium into the cytosolic space triggers various intracellular signaling pathways and downstream effects (Negi et al., 2023). When plants encounter environmental changes, the initial response involves an intracellular shift in free Ca^{2+} levels, initiating a signaling cascade critical for adaptive responses (Tong et al., 2021). These triggers activate calcium-permeable channels in the plasma membrane (e.g., OSCA, MCA, CNGC, GLR) or intracellular stores like the endoplasmic reticulum and vacuoles, generating

rapid Ca^{2+} influx and distinct spatiotemporal “calcium signatures” that encode information about stimulus type, strength, duration, and location (Tian et al., 2020; Thor et al., 2020). Under mechanical stress, such as root bending, soil compaction, or touch, plants exhibit rapid, biphasic Ca^{2+} spikes in $[\text{Ca}^{2+}]_{\text{cyt}}$ within seconds, with amplitudes and recovery kinetics that often attenuate with repeated stimuli, indicating dynamic adaptation (Thor et al., 2020). These mechanical Ca^{2+} signals propagate as intercellular waves, facilitated by plasmodesmata and ROS–RBOH feedback loops, integrating local mechanical sensing into systemic responses (Fichman & Mittler, 2020). Calcium signaling is ubiquitous across stress responses but is particularly prominent in mechanical stress, serving as one of the earliest and most rapid biochemical indicators of physical perturbation (Tian et al., 2020). These calcium signatures are decoded by Ca^{2+} -binding sensors, including calmodulins (CaMs), calmodulin-like proteins (CMLs), calcium-dependent protein kinases (CDPKs), and calcineurin B-like proteins (CBLs) interacting with CBL-interacting protein kinases (CIPKs), which activate downstream pathways such as MAPK cascades, ROS production, gene expression, and alterations in hormone levels and cell wall structure (Kudla et al., 2018; Thor et al., 2020). The abundance and diversity of plant Ca^{2+} sensors, channels, and transporters highlight the expansive toolkit that enables the translation of Ca^{2+} signals into specific physiological responses (Luan and Wang, 2021; Dong et al., 2022).

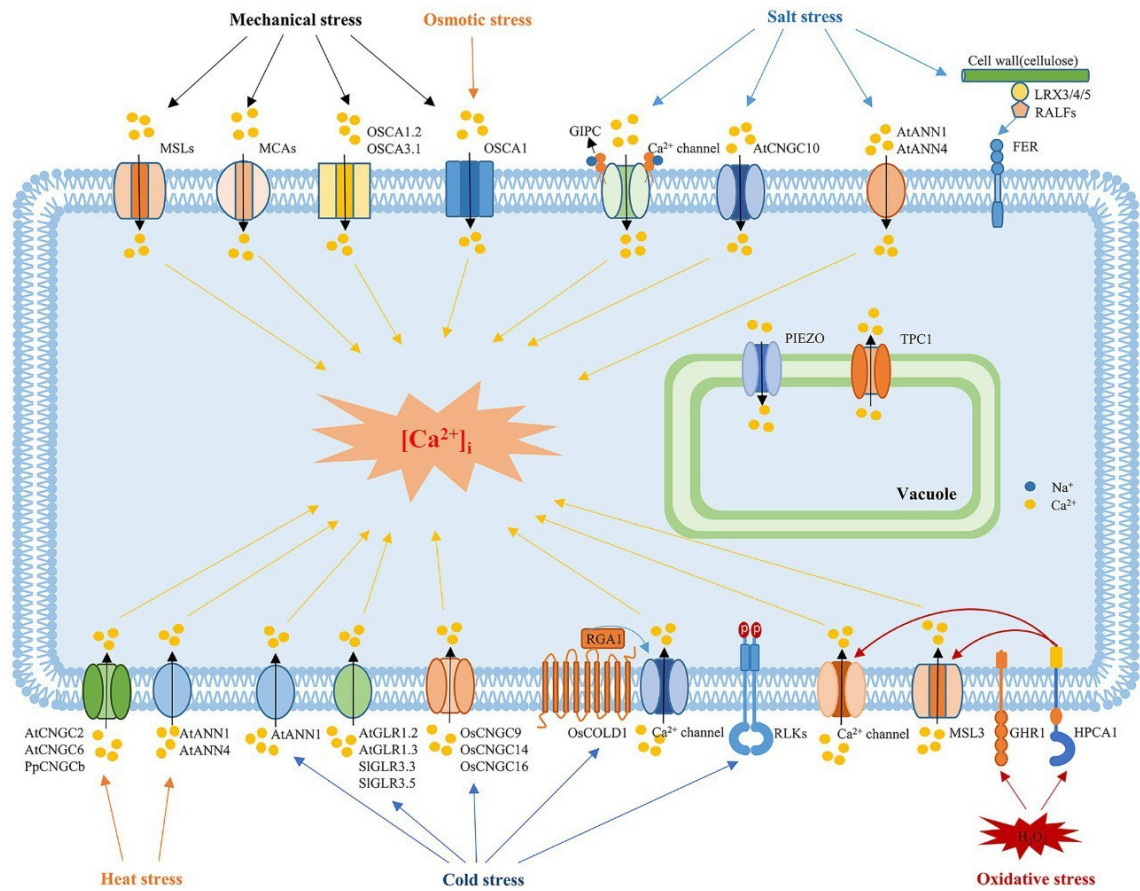


Figure 2. Calcium signaling serves as a vital lifeline for plants, activating to help them respond to a range of challenging conditions, including the gentle nudge or firm push of mechanical stress. When such pressure is encountered, specialized channels like MSLs, MCA, Piezos, and OSCAs come to life, graciously allowing calcium ions to flow into the cell. MCA and OSCA are stationed along the plasma membrane, while Piezo stands guard at the vacuole membrane. OSCA1, a key sentinel on the cell surface, acts as a responsive gate, opening to permit calcium entry and initiate the critical rise in intracellular calcium ($[Ca^{2+}]_i$) when mechanical stress is detected (Singh et al., 2022).

1.10 Calcium-Dependent Protein Kinase (CDPK/CPK) Family

Calcium-dependent protein kinases (CDPKs or CPKs) constitute a large family of sensor-effector proteins in plants, characterized by a unique structure that integrates a serine/threonine kinase domain with a C-terminal calmodulin-like domain containing four EF-hand Ca^{2+} -binding motifs. (Kudla et al., 2018). CDPKs are calcium-regulated protein kinases that transduce calcium signals by directly phosphorylating transcriptional regulators

like MYB, MYC, etc. leading to altered gene expression .For example, rice CDPK7 phosphorylates and activates OsMYB2 involved in cold tolerance (Naz et al., 2024).) In *Arabidopsis thaliana*, this family encompasses 34 members, categorized into four major subfamilies based on sequence similarity, expression patterns, and regulatory features. Each CDPK typically comprises an N-terminal variable region that determines subcellular localization and partner specificity, a kinase domain responsible for catalyzing phosphorylation, an autoinhibitory junction, and a Ca²⁺-binding calmodulin-like domain that triggers activation upon calcium binding (Kudla et al., 2018). Specialized Ca²⁺ sensor proteins like CDPKs detect transient Ca²⁺ signatures, decoding the signal through conformational changes that activate downstream response cascades (Köster et al., 2022). Downstream of the calcium elevation, calcium-binding proteins decode the calcium signature to activate signaling kinase cascades involving CDPKs. (Boudsocq and Sheen, 2013).

1.10.1 Interaction in Stress Signaling

Calcium-dependent protein kinases (CDPKs) are pivotal decoders of Ca²⁺ signatures elicited under stress conditions, undergoing conformational activation (figure 3) upon cytosolic Ca²⁺ increases to phosphorylate diverse downstream targets, including ion channels, NADPH oxidases (RBOHs), transcription factors (e.g., ABF1/4, WRKYs), and other kinases, thereby engaging in intricate crosstalk with MAPK pathways, hormone signaling, and ROS production (Boudsocq & Sheen, 2013). For instance, truncated tobacco CDPK2 activates ROS production, ethylene, and jasmonate synthesis while attenuating MAPK signaling, demonstrating CDPKs' ability to both synergize with and modulate other signaling pathways (Ludwig et al., 2005). In *Arabidopsis*, CPK5, CPK6, and CPK11 regulate early gene expression and ROS bursts through RBOHD phosphorylation, playing a critical role in innate immunity (Boudsocq & Sheen, 2013).

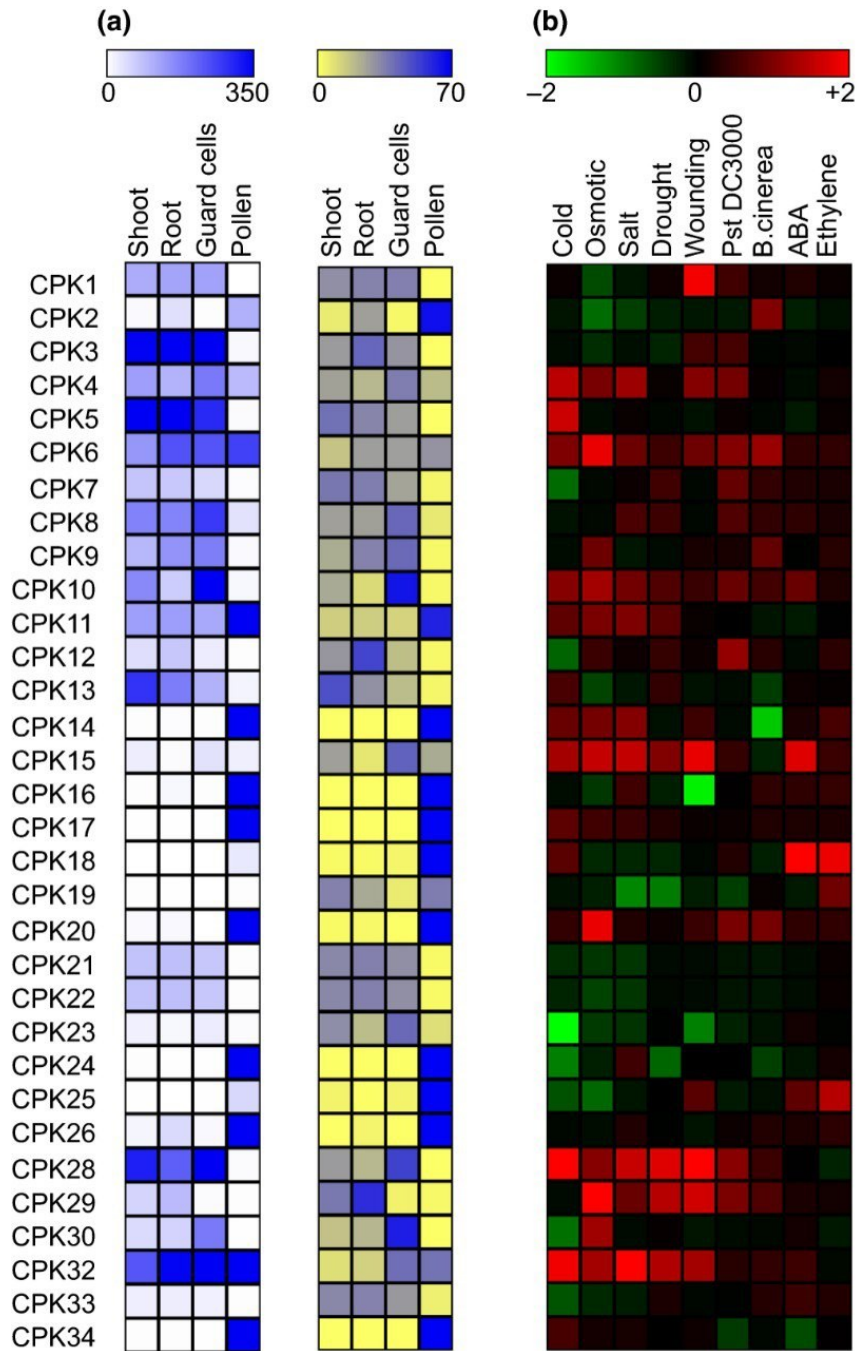


Figure 3. Activity Snapshot of Arabidopsis CPKs. (a) This illustration presents the expression profiles of Arabidopsis CPK proteins across various organs and cell types, meticulously collected from the eFP Browser (left panel) and thoughtfully normalized as a percentage of total expression for each CPK (right panel). This normalization gracefully highlights the leading CPK in each organ while tenderly unveiling the subtle expression patterns of less prominent CPKs. (b) The expression patterns of Arabidopsis CPKs in response to a range of abiotic and biotic treatments are carefully compiled from the eFP Browser, though data remains unavailable for AtCPK27 and AtCPK31. (Schulz et al., 2020)

1.10.2 CDPK Subfamilies, Members, and Stress Roles

CDPKs in plants are classified into four subfamilies (figure 4), each exhibiting functional specialization. Subfamily I, including AtCPK4, AtCPK5, AtCPK6, and AtCPK11, is primarily involved in abiotic stress responses (e.g., drought, salinity) and pathogen defense, notably through ABA signaling via phosphorylation of ABF transcription factors (Boudsocq & Sheen, 2013). Subfamilies II–IV encompass CDPKs associated with developmental processes, such as pollen tube growth and root elongation, as well as responses to heavy metal or temperature stresses across species, exemplified by OsCPK13 in rice and StCDPK4/5 in potato (Simeunovic et al., 2016). Additionally, CPK5 mediates PAMP-triggered immunity and ROS generation, while CPK6 contributes to stomatal closure and drought responses through guard-cell signaling (Boudsocq & Sheen, 2013). CDPKs are thus integral to a broad spectrum of stresses—abiotic (e.g., cold, drought, salt, heat, heavy metals), biotic (e.g., pathogens, herbivores), and developmental cues—via phosphorylation of substrates that regulate ion fluxes, gene expression, and oxidative responses (Simeunovic et al., 2016).

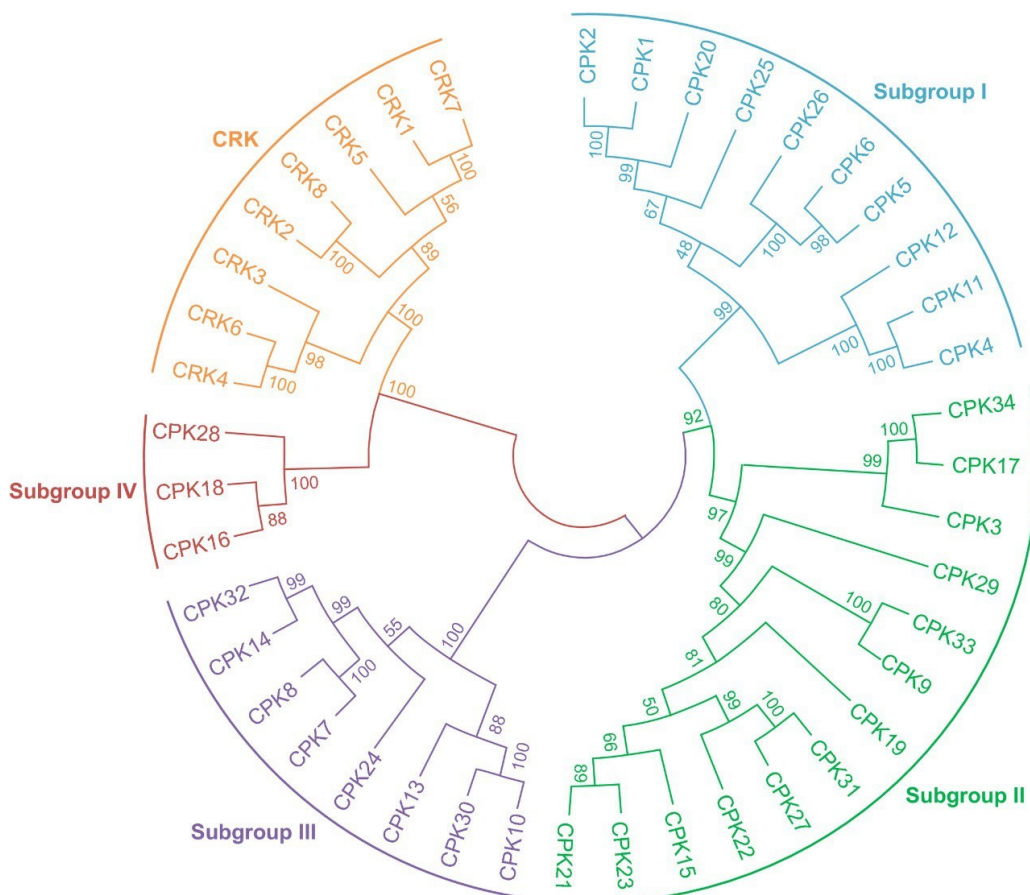


Figure 4. Family Tree of Arabidopsis CPKs. This visual map showcases the relationships among Arabidopsis thaliana CPK proteins, crafted using MEGA 7 software with the neighbor-joining method and fortified by 1000 bootstrap replicates for reliability. The CPK family, affectionately known as CDPKs, branches out into four distinct subgroups (I–IV), each

representing a unique lineage (Schulz et al., 2020).

1.11 Candidate genes for Mechanical Stress Regulation in Root Hairs

Members of the Calcium-Dependent Protein Kinase (CPK) family exhibit tissue-specific expression, activation patterns, and functional roles, with CPK4 and CPK11 being among the most highly expressed isoforms in *Arabidopsis thaliana* root hairs, positioning them as prime candidates for investigating mechanical stress responses in these cells (Yip Delormel & Boudsocq, 2019). Firstly, CPK11 is transcriptionally regulated by root hair master regulators, with evidence demonstrating that it is a direct downstream target of RSL4, a transcription factor critical for root hair elongation. Mutants lacking CPK11 produce significantly shorter root hairs, while its overexpression does not induce unintended phenotypic effects, indicating a specific role in tip-growth calcium signaling in root hair cells (Yip Delormel & Boudsocq, 2019). Secondly, gene expression data from the Root Cell Atlas dataset (rootcellatlas.org) confirm that both CPK4 and CPK11 are strongly expressed in root hair cells, particularly in the root hair differentiation zone, consistent with their reported roles in regulating root growth and hair development (Yip Delormel & Boudsocq, 2019). Thirdly, CPK4 and CPK11 exhibit functional redundancy in various stress signaling contexts, including abscisic acid (ABA) responses, salt tolerance, hydrotropism, and metal stress. For example, *Arabidopsis cpk4* mutants display insensitivity to drought and salt, with double mutants (*cpk4/cpk11*) enhancing these phenotypes, indicating overlapping roles in stress responses (Zhu et al., 2007).

2. AIM OF THE STUDY

This study aims to investigate the roles of calcium-dependent protein kinases (CPKs), specifically CPK4 and CPK11, in the mechanosensory signaling pathways of root hairs, focusing on their functions and potential interactions with ANNEXIN1 in response to mechanical stress. Root hairs play a critical role in plant interaction with the soil, yet how they adapt to mechanical challenges like drought or compacted soil remains an area of active research. While previous work has documented morphological changes, such as reduced root hair growth under elevated agar concentrations (Pereira et al., 2024) or water scarcity (Haling et al., 2013), the precise molecular mechanisms enabling root hairs to sense and respond to physical cues are not fully elucidated. This study aimed to bridge that knowledge gap by pinpointing key regulatory components involved in root hair mechanosensation.

Our investigation specifically focused on the calcium-dependent protein kinases, CPK4 and CPK11, alongside ANNEXIN1, a protein previously implicated in calcium transport and root development. Although the CDPK family is broadly recognized for its role in abiotic stress responses (Atif RM et al., 2019), their involvement in perceiving mechanical stress has been largely unexplored. To address these gaps, this research is guided by several key questions. First, we will ask: What functional roles do CPK4 and CPK11 play in the mechanosensory signaling pathways in root hairs. Second, we will consider: How similar or different are the functions of CPK4 and CPK11, given their close relation within the CDPK gene family. Finally, we will explore: Does ANNEXIN1 interact with or regulate the activity of CPK4 and CPK11 in response to mechanical stress signals, investigating whether this calcium-binding protein physically interacts with or modulates their activity. Through addressing these questions, this research aims to provide a comprehensive understanding of CPK4 and CPK11 functions in root hair mechanosensory signaling, their potential interplay with ANNEXIN1, and their contributions to plant resilience under mechanical stress, with broader implications for crop improvement.

3. Material and Methods

3.1 Development of Root Hair Isolation Methods

Two distinct root hair isolation methods were developed and tested in parallel to selectively extract root hairs from *Arabidopsis thaliana* seedlings.

3.1.1 Cryo-mechanical disruption

Excised roots were divided into two sets (7 and 15 seedlings) and transferred into 1.5 mL microcentrifuge tubes. Samples were flash-frozen in liquid nitrogen for 10 seconds, then immediately agitated in a Qiagen TissueLyser at 30 Hz for 1 minute without beads. This freeze-agitate step was repeated twice. The agitation generated sufficient shear force to detach root hairs while leaving the main root intact, allowing for easy separation of the hairless roots. This approach is illustrated in the graphical abstract (Figure 5).

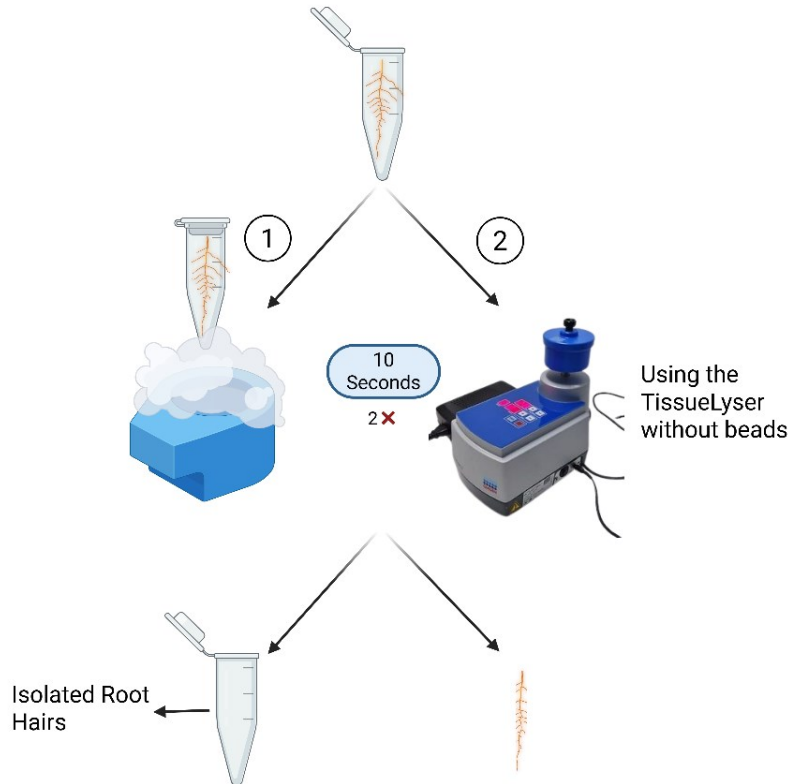


Figure 5. Schematic of the cryo-mechanical disruption method for root hair isolation. (1) Liquid nitrogen. (2) TissueLyser (Biorad, USA). Figure created with BioRender.com.

3.1.2 The freeze-thaw lysis

Roots were also divided into two sets (7 and 15 seedlings) and submerged in 100 μ L of RLT buffer (Qiagen RNeasy Plant Mini Kit) for 1 minute to promote loosening of root hairs. Samples underwent two freeze–thaw cycles: 10 seconds in liquid nitrogen followed by 10 seconds in a 37 °C water bath. A brief vortex aided in detachment, after which the lysates were centrifuged at 12,000 \times g for 1 minute. The root hair-containing supernatant was collected, and the pelleted hairless roots were discarded. This approach is illustrated in the graphical abstract (Figure 6).

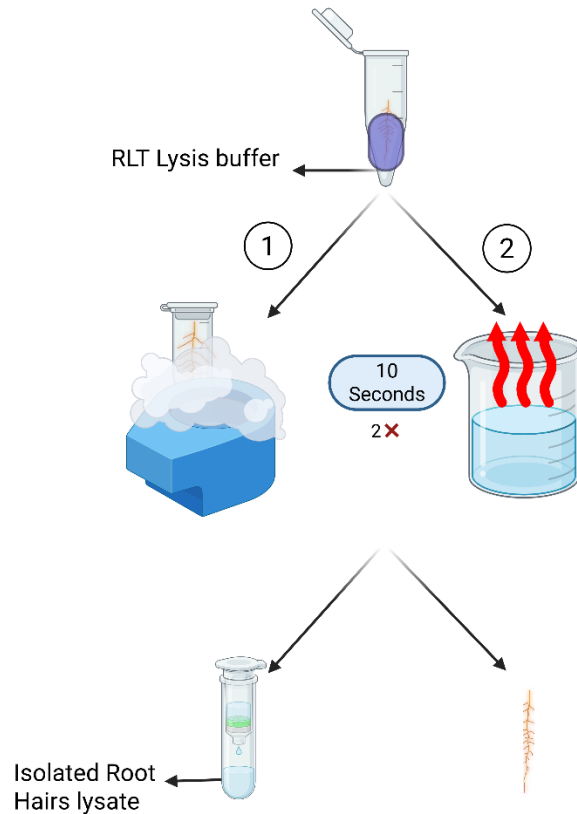


Figure 6. Schematic of the freeze-thaw lysis method for root hair isolation. (1) Liquid nitrogen. (2) Hot water (47°C). Figure created with BioRender.com.

3.1.3 Validation of Root Hair Isolation

To evaluate the specificity and efficacy of both root hair isolation methods, a combination of microscopic, spectrophotometric, and molecular techniques was employed.

3.1.4 Microscopic Validation

Visual confirmation of successful root hair removal was performed by imaging roots before and after isolation using stereomicroscopy (Zeiss Discovery V.8) and differential interference contrast (DIC) microscopy (Leica DM6 B). These methods provided both overview and high-resolution visualization, confirming the effective detachment of root hairs while preserving the root axis.

3.1.5 Gel-Based RNA Quality Assessment

Total RNA was extracted from all samples using the RNeasy Plant Mini Kit (Qiagen), incorporating an DNase I treatment (Thermo Fisher Scientific) to eliminate genomic DNA contamination. RNA integrity was further verified by electrophoresis on 1.5% agarose gels, confirming the presence of sharp 18S and 28S rRNA bands.

3.1.6 Molecular Marker Validation

For functional validation, 1 µg of total RNA was reverse transcribed using the iScript cDNA Synthesis Kit (Bio-Rad, USA). PCR amplification targeted both root-specific markers (SCR [AT3G54220], SHR [AT4G37650]) and root hair-specific markers (EXP7 [AT1G12560], RSL4 [AT1G27740]) Primers were designed to span exon–exon junctions to ensure specificity for mature transcripts (Table 2).

Gene	AGI Code	Forward Primer (5'–3')	Reverse Primer (5'–3')
RSL4	AT1G27740	CAGTTGACGAGAGCAACACT	CTTCTCTCTTCGTTTCCGAGC
EXP7	AT1G12560	TGCATACCGAAGAGTGCCAT	CCAATTCGTCCGGCTACCTT
SCR	AT3G54220	AAGGGAAGCTGTGGCTGTTCAC	AGTGTGTGCATCAGAGCCAGTG
SHR	AT4G37650	AGGGTTTGCTTCGAGTCATGGG	TGCACGCTCTAGCATCAACCTC

Table 1. Primer Sequences for Root-Specific and Root Hair-Specific Markers. This table provides the primer sequences for root-specific markers, including Scarecrow (SCR, AT3G54220) and Short-Root (SHR, AT4G37650), as well as root hair-specific markers, comprising Expansin7 (EXP7, AT1G12560) and Root Hair Defective6-Like4 (RSL4, AT1G27740). The primers were meticulously designed to span exon–exon junctions, ensuring high specificity for mature transcripts.

The amplified products were resolved on 1.5% agarose gels to confirm the enrichment of root hair-specific transcripts and the absence or reduction of whole-root signals, supporting the specificity of the isolation procedures.

3.2 In Silico Analysis of Mechanosensitive Genes and Stress Responses

To identify candidate genes potentially involved in mechanical stress responses in *Arabidopsis thaliana*, an extensive literature review and database search were conducted. Gene families previously reported to play roles in mechanotransduction—such as calcium-dependent protein kinases (CDPKs), annexins, mechanosensitive ion channels, and cytoskeletal regulators—were curated based on publications indexed in PubMed and functional annotations available from The Arabidopsis Information Resource (TAIR).

Expression profiling of these gene families was carried out using the ePlant platform (<https://bar.utoronto.ca/eplant/>) with a focus on *root tissue*-specific data. Transcript abundance under various abiotic stress conditions—including drought, salinity, cold, heat, osmotic stress, and mechanical stimuli—was visualized using the integrated datasets from Kilian et al. (2007). Specifically, the "Abiotic Stress" experiment from this study, based on root microarray data, enabled a high-resolution analysis of spatial and stress-induced expression patterns. Heatmaps were generated to compare the expression of each gene family member, allowing for the identification of root-expressed mechanosensitive genes with consistent upregulation under stress conditions.

3.3 Root Cell-Type Specific Expression Analysis via RootCellAtlas

To identify CDPK gene family members with potential roles in mechanical stress response within root hair cells, spatial gene expression data were examined using the RootCellAtlas platform (<https://www.rootcellatlas.org>). This tool enables high-resolution analysis of gene expression across individual root cell types in *Arabidopsis thaliana*, including root hair cells, atrichoblasts, and cortical layers. Each CDPK family member was queried to evaluate its relative abundance in epidermal tissues.

A total of 34 CDPK genes were analyzed, and individual expression plots were downloaded for documentation. Genes showing strong expression specifically in root hair cells were shortlisted for further functional evaluation. A summary heatmap was constructed using normalized expression values across cell types and visualized using the pheatmap package in R (version 4.3.1), allowing for clustering based on expression patterns.

3.4 RNA-seq Analysis of Compacted Soil Stress in Rice Roots

3.4.1 Differential Gene Expression and Filtering

Differentially expressed genes (DEGs) were obtained from a published RNA-seq study comparing rice roots under compacted versus control soil conditions (Zhu et al. (2025)). Raw count data were analyzed using DESeq2 (v1.34.0) in R (v4.2.1), with normalization via the median-of-ratios method. Genes with $|\text{Log}_2\text{FC}| \geq 1$ and $\text{FDR} \leq 0.05$ were considered differentially expressed.

To focus on relevant genes, DEGs were filtered based on tissue-specific expression using data from the Rice Genome Annotation Project (<http://rice.uga.edu>). Genes predominantly expressed in roots were prioritized due to the direct impact of soil compaction on root growth. Filtered DEGs were divided into upregulated ($\text{Log}_2\text{FC} \geq 1$) and downregulated ($\text{Log}_2\text{FC} \leq -1$) groups. Results were compiled into CSV files containing LOC IDs, Log_2FC , FDR values, and root expression data.

3.4.2 GO Annotation and Arabidopsis Homologs

Functional annotations for DEGs were retrieved from the Rice Genome Annotation Project, including Gene Ontology (GO) terms for biological processes, molecular functions, and cellular components. To identify Arabidopsis homologs, rice coding sequences were aligned to the TAIR10 protein database using BLASTP (E-value $\leq 1e-5$). The best hit for each gene was selected, and functional similarity was confirmed through GO term comparison.

Expression patterns of Arabidopsis homologs were visualized using the ePlant platform (<https://bar.utoronto.ca/eplant>). Log_2FC values, either from Arabidopsis datasets or inferred from rice, were used to create a heatmap showing upregulated and downregulated genes. Hierarchical clustering based on Euclidean distance revealed co-expression trends, highlighting conserved responses to mechanical stress.

3.5 QTL Mapping of Mechanosensory Candidates Using AraQTL

To explore potential co-regulated or functionally associated genes with *CPK4*, *CPK11*, we performed quantitative trait loci (QTL) mapping using the AraQTL platform (<https://www.bioinformatics.nl/AraQTL/>). This tool leverages expression and phenotype datasets derived from the *Arabidopsis thaliana* 1001 Genomes Project to identify expression QTLs (eQTLs) and regulatory relationships. Using the gene IDs corresponding to *CPK4*(*AT4G09570*) and *CPK11*(*AT1G35670*), co-expression modules and QTL intervals were explored to uncover genes with overlapping regulatory loci or expression profiles.

3.6 Plant Material and Experimental Conditions

This study utilized four *Arabidopsis thaliana* genotypes: the wild-type Columbia-0 (Col-0) and three T-DNA insertional knockout lines, *CPK4* (SALK_081860C), *CPK11* (SALK_054495C), and *ANNEXIN1* (SALK_132169C). Seeds were obtained from the Arabidopsis Biological Resource Center (ABRC), and homozygosity of each mutant line was confirmed using gene-specific and T-DNA border primers (Table1) provided by the ABRC, following their recommended PCR genotyping protocols.

Seeds were stratified at 4 °C in darkness for three days to synchronize germination and then sown on ½-strength Murashige and Skoog (MS) medium. Plants were grown vertically under controlled environmental conditions: 16-hour light / 8-hour dark photoperiod at 21 ± 1 °C. Illumination was supplied by cold white fluorescent lamps with a photon flux density of 70–80 μmol·m⁻²·s⁻¹. Relative humidity was maintained at ≥75% throughout the growth period.

T-DNA Line	Gene	Forward Primer (LP) (5'→3')	Reverse Primer (RP) (5'→3')	BP+RP Product Size
SALK_081860C	<i>CPK4</i>	TTTTTGGTCGAGTCTGATTGG	TCCTTGAACCAACCAACAAAG	595–895 bp
SALK_132169C	<i>ANNEXIN1</i>	GCCTGCTTCAGCTTTTGTATG	AACGCTACCGACACAACATTC	443–743 bp
SALK_054495C	<i>CPK11</i>	TTGCAATGTCACTAATTAACAAACC	AAACCAATTAGGCGATGAACC	432–732 bp

Table 2. Primer sequences used for genotyping T-DNA insertion lines. LBb1.3 primer (Newly used by Salk Genotyping Project and with better results) (ATTTTGCCGATTTTCGGAAC).

3.7 Root Hair Phenotyping

Seeds were surface-sterilized by immersion in 70% ethanol for 5 minutes, followed by treatment with 1% sodium hypochlorite for 10 minutes. They were then rinsed five times with sterile distilled water. Stratification was performed at 4 °C in darkness for three days to synchronize germination. Sterilized seeds were subsequently sown onto ½-strength Murashige and Skoog (MS) medium supplemented with MES buffer (Duchefa, Netherlands) and solidified with Plant Agar™ (Duchefa, Netherlands) at five different concentrations (0.5%, 0.8%, 1.0%, 1.25%, or 1.5% w/v). The media were poured into 120 × 120 mm square Petri dishes (Greiner, Austria).

To simulate soil compaction, seeds were gently pressed into the solidified agar surface using the tip of a sterile syringe, ensuring minimal disruption to the medium. Seedlings were grown vertically under controlled conditions for 10 days (Figure7).

Root hair phenotyping was carried out by imaging the root zones using a Zeiss Discovery V.8 stereomicroscope. For each seedling (n = 5 per condition), five fully elongated root hairs were manually measured using ImageJ software. The mean root hair length was calculated for each sample, and results were expressed as mean ± standard deviation (SD). Statistical analyses and graphical representations were performed using GraphPad Prism version 10.4.2 (GraphPad Software, USA).

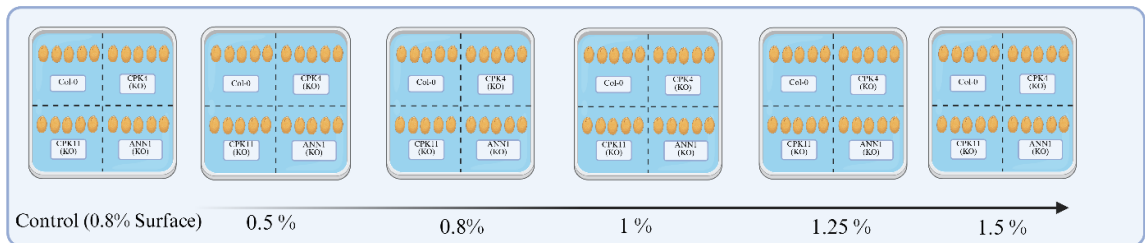


Figure 7. Schematic representation of growth assays on agar plates with varying concentrations (0.5%, 0.8%, 1%, 1.25%, 1.5%). Col-0, CPK4, CPK11, and ANNEXIN1 lines were embedded in the medium, while a control (0.8% agar) featured the same lines placed on the surface.

3.8 RT-PCR and RT-qPCR

Root hairs from 10-day-old *Arabidopsis* seedlings (*Col-0*, *CPK4 KO*, *CPK11 KO*, and *ANNEXINI KO* under both stress and control conditions) were isolated using the freeze–thaw cycle method. Total RNA was extracted using the RNeasy Plant Mini Kit (Qiagen), including on-column DNase I treatment (Thermo Fisher Scientific) to remove genomic DNA contamination.

For reverse transcription, 1 µg of total RNA was used as input for cDNA synthesis with the iScript™ cDNA Synthesis Kit (Bio-Rad, USA; Cat. No. 1708891). Quantitative real-time PCR (RT-qPCR) was performed using the iQ™ SYBR® Green Supermix (Bio-Rad, USA; Cat. No. 170882) on a Bio-Rad CFX Connect™ Real-Time PCR Detection System, following the manufacturer’s instructions.

Primers were designed to span exon–exon junctions to ensure specificity for mature transcripts (Table 3). The expression of target genes (*CPK4*, *CPK11*, and *ANNEXINI*) was analyzed, with *AT8* serving as the reference gene for normalization.

Gene	AGI Code	Forward Primer (5'–3')	Reverse Primer (5'–3')
CPK4	AT4G09570	ATGAAGCATTGTGTACCCCT	CACCAATCTCTCCTCCGAG
CPK11	AT1G35670	GGCATTACGGGTAATTGCTG	TATCAGCCGCATCCATGAG
ANNEXIN1	AT1G35720	GTCGGCTTCGACTCCCAACAT	CCTCGTTCGTACCCCATCCTTC
ACT8 (control)	AT1G49240	GATCACAGCTCTTGCCCCGA	GGACAATGCCTGGACCTGCT

Table 1. Primer Sequences for target Genes. This table lists primer sequences designed using Primer-BLAST in NCBI to span exon–exon junctions, ensuring specificity for mature transcripts

4. Results

4.1 Development and Validation of Root Hair Isolation Methods

4.1.1 Method Efficiency and Visual Validation

Both root hair isolation methods, cryo-mechanical disruption (Figure 8A) and freeze-thaw lysis (Figure 8B), successfully detached root hairs, as confirmed by stereomicroscopy and DIC imaging.

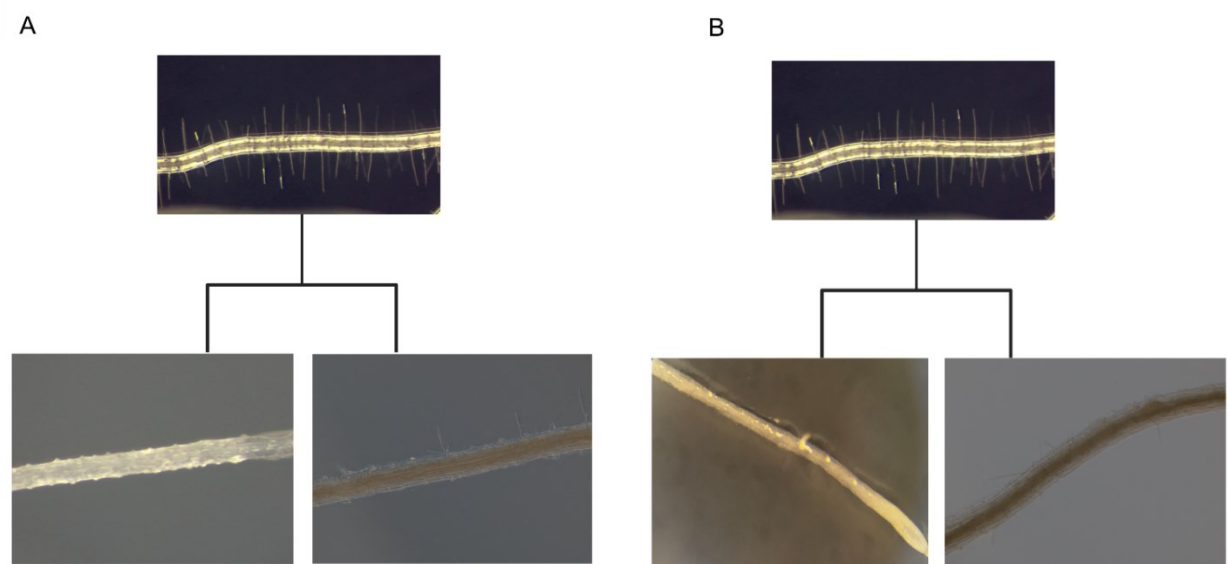


Figure 8. Visualization of Root Hair Detachment via Cryo-Mechanical and Freeze-Thaw Techniques. (A) Cryo-mechanical disruption and (B) freeze-thaw lysis effectively detached root hairs, validated through stereomicroscopy (lower left) and Differential Interference Contrast (DIC) microscopy.

4.1.2 RNA Yield and Quality

RNA extracted from isolated hairs showed lower total yields ($\sim 20\text{-}40\text{ng}/\mu\text{L}$) compared to whole roots ($\sim 50\text{-}150\text{ ng}/\mu\text{L}$), consistent with selective sampling. Spectrophotometric ratios

(A260/280 and A260/230) were within acceptable purity ranges, and gel electrophoresis confirmed RNA integrity (Figure 9).

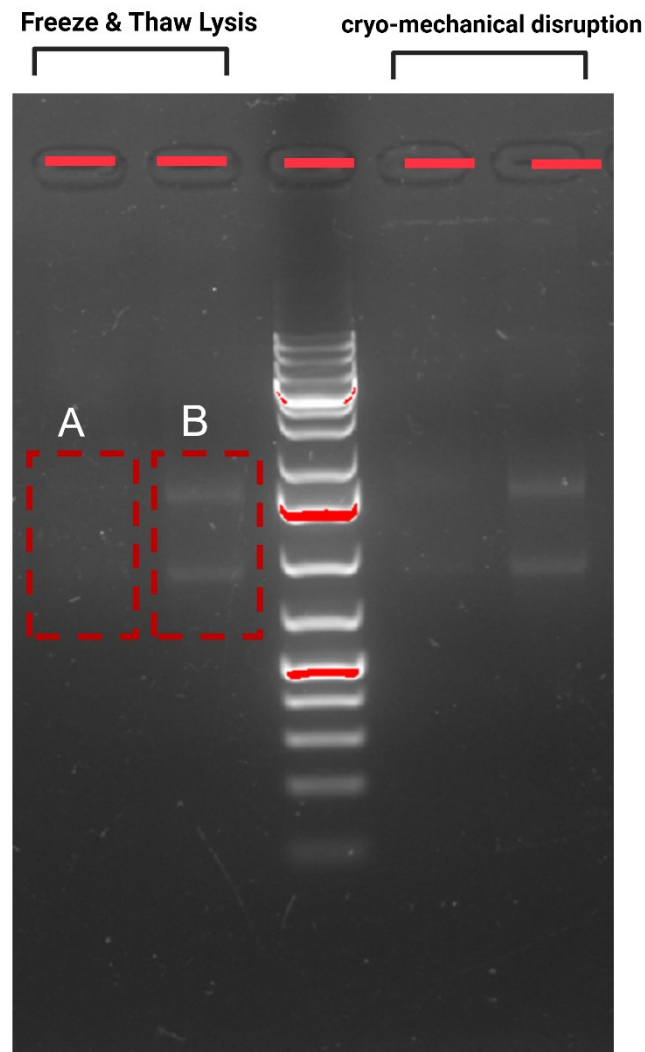


Figure 9. Agarose Gel Electrophoresis of RNA from Isolated Root Hairs and Whole Roots. This image displays the RNA integrity from (A) approximately 8 seedlings used for root hair isolation and RNA extraction, and (B) approximately 16 seedlings used for root hair isolation and RNA extraction, with clear visualization of 18S and 28S rRNA bands indicating RNA quality.

4.1.3 Marker-Based Validation of Hair Specificity

PCR validation showed enrichment of root hair markers (EXP7, RSL4) in isolated samples and depletion of non-hair/root markers (SCR, SHR), confirming successful specificity (Figure 10).

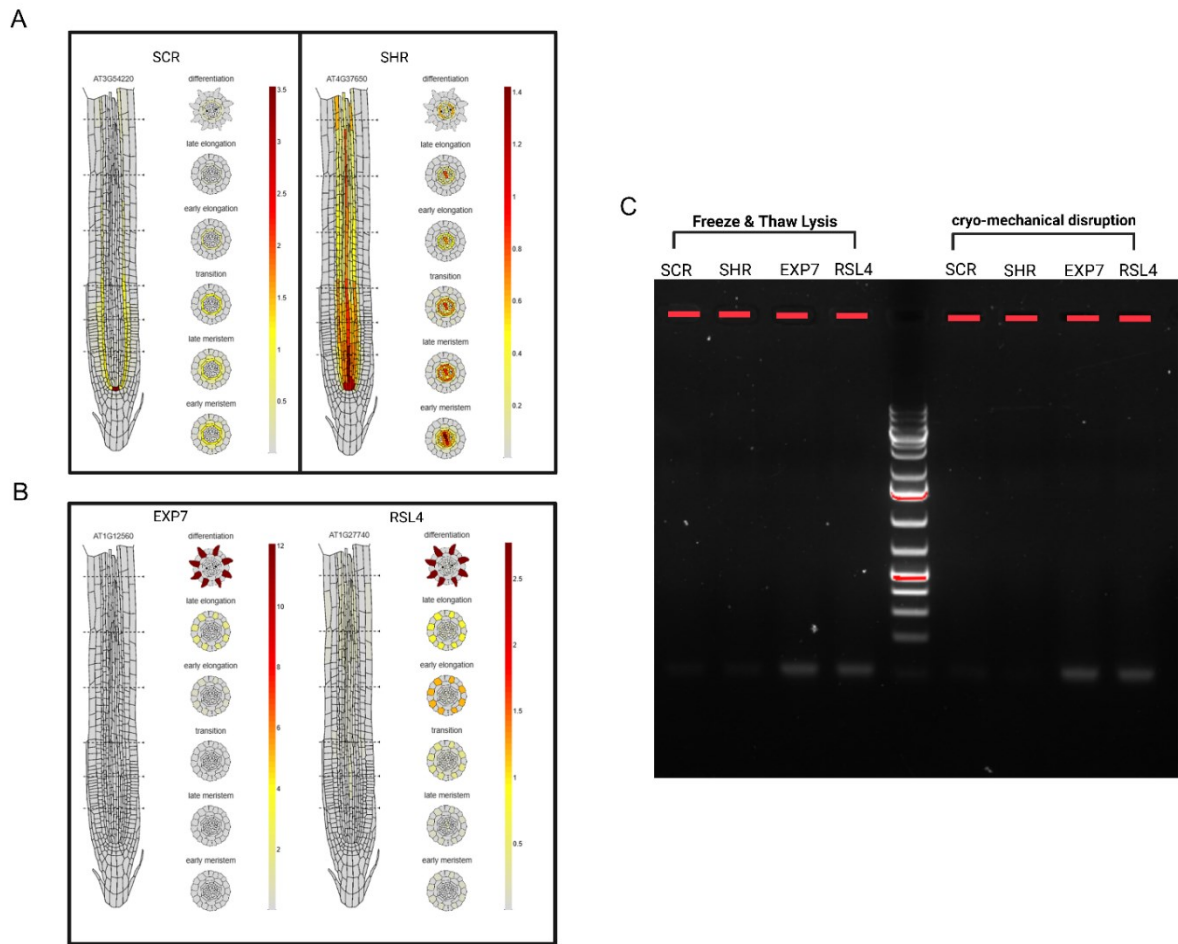


Figure 10. Agarose Gel Analysis of PCR Products from Root-Specific and Root Hair-Specific Markers. This image presents the results of PCR amplification, with (A) targeting root-specific markers SCR (AT3G54220) and SHR (AT4G37650), and (B) focusing on root hair-specific markers EXP7 (AT1G12560) and RSL4 (AT1G27740). The agarose gel visualizes PCR products from isolated root hairs and hairless roots, confirming marker specificity.

4.2 In Silico Analysis of Mechanosensitive Genes and Stress Responses

Our journey to understand how plants sense mechanical stress began with an extensive survey of published research, where we identified key players in this biological process (see complete list in Supplementary Table 4). Using the powerful ePlant analysis tool from the University of Toronto, we then tracked how these genes behave when plants face various challenges - from drought and salt to physical damage and temperature extremes.

The heatmap we generated (Figure 11) tells an interesting story about root responses. Some genes sprang into action across nearly all stress conditions, like general first responders. Others were more specialized, only reacting to certain threats. The timing of gene activation varied too - some responded immediately while others showed delayed reactions. Particularly noteworthy were genes involved in calcium signaling and cell wall modification, which showed strong

responses to both water-related stresses and physical pressure, hinting at their possible dual role in helping root hairs navigate through tough soil conditions.

Table 2. Comprehensive List of Mechanosensitive Genes Identified in Published Research. This table compiles the key mechanosensitive genes involved in plant stress responses, identified through an extensive survey of published literature, providing a detailed reference for further analysis.

Category	Genes
Mechanosensitive Ion Channels	MSL2, MSL3, MSL8, MCA1, MCA2, TCH3, ANNEXIN1, ANNEXIN2, ANNEXIN4, ANNEXIN5, CNGC14, PZO1 (PIEZO1)
Calcium Signaling Components	CDPK/CPK, CBL1, CBL9, CIPK6, CIPK23, HPCAL1, HPCAL2, HPCAL4, CAMTA3
Proton Pumps & pH Regulation	AHA1, AHA2, AHA7, VHA-A1, VHA-B2, CHX17, CHX20
Reactive Oxygen Species (ROS) Production & Signaling	RBOHA, RBOHB, RBOHC, RBOHD, RBOHF, PRX33, PRX34, CSD1, CSD2, FSD1
Actin Cytoskeleton & Cell Wall Remodeling	ACT2, ACT7, ACT8, MYA1, MYA2, MYO11B, SCAR2, SCAR4, BRK1, ROP2, ROP6, ROP10, XTH17, XTH18, XTH19, FLA11, FLA12, TUA6, MAP65-1, PMIR1, PMIR2
Hormonal Regulation in Mechanical Stress Response	AUX1, PIN1, PIN2, PIN3, PIN7, EIN2, EIN3, ETR1, ETR2, ERS1, ERS2, MYC2, JAZ1, JAZ10, ERF1, ASA1, ASB1, PP2A B (interacts with VIP1 regulating ABA catabolism)
Transcription Factors Involved in Mechanosensing	WRKY33, WRKY40, WRKY46, ERF109, ERF115, MYB77, MYB73, BES1, BZR1
Microtubule-Associated Proteins	WDL5, WDL6, KATANIN, CLASP, NEK6, MAP65-1, CLASP
Receptor-Like Kinases	BAK1, FERONIA (FER), THESEUS1 (THE1), MIK2/LRR-KISS
Thigmomorphogenesis and Touch-Responsive Genes	TCH1, TCH2, TCH3, TCH4, TREP1, EXO70H4

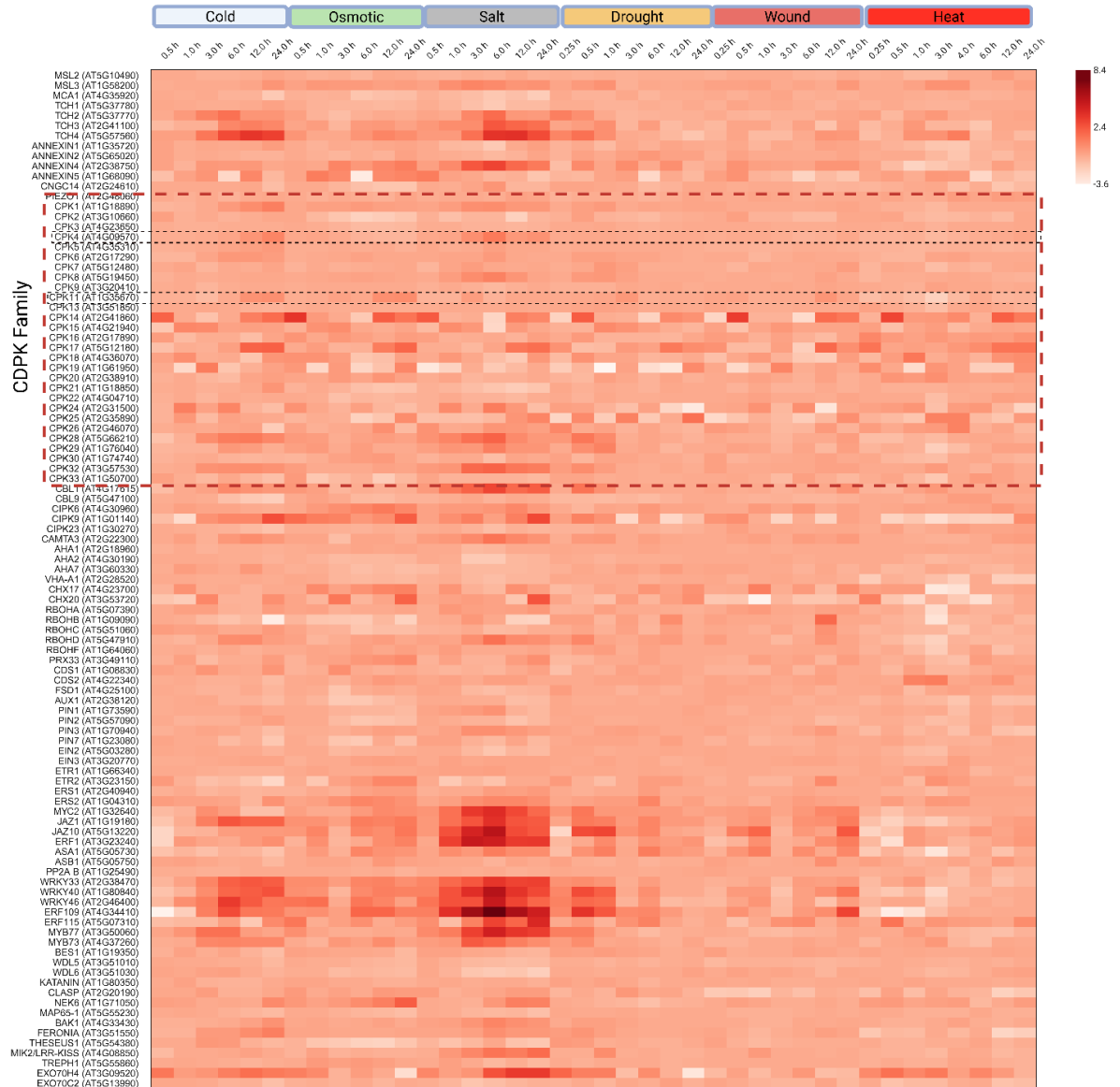


Figure 11. Heatmap of Mechanosensitive Gene Expression Across Stress Conditions. This heatmap, generated using BioRender.com, illustrates the expression patterns of mechanosensitive genes in roots under diverse, with data sourced from the ePlant analysis tool.

4.3 Root Hair Cell-Type Specific Expression (RootCellAtlas)

To pinpoint which calcium-sensing genes might control root hair growth, we turned to the RootCellAtlas, a detailed map of gene activity in different root cells. Among the 34 members of the CDPK family (grouped into four evolutionary branches, Figures 12–15), two genes stood out: CPK4 and CPK11. These genes were especially active in root hairs compared to other cell types (Figure 16), hinting at a specialized role in hair formation.

Digging deeper, we found that both genes were most active during the differentiation stage, the phase where root hairs start elongating and encountering physical resistance from the soil (Figure 16). Since this is when root hairs experience mechanical stress, CPK4 and CPK11 might help cells sense and respond to these external forces, given their strong expression in root hairs at this stage.

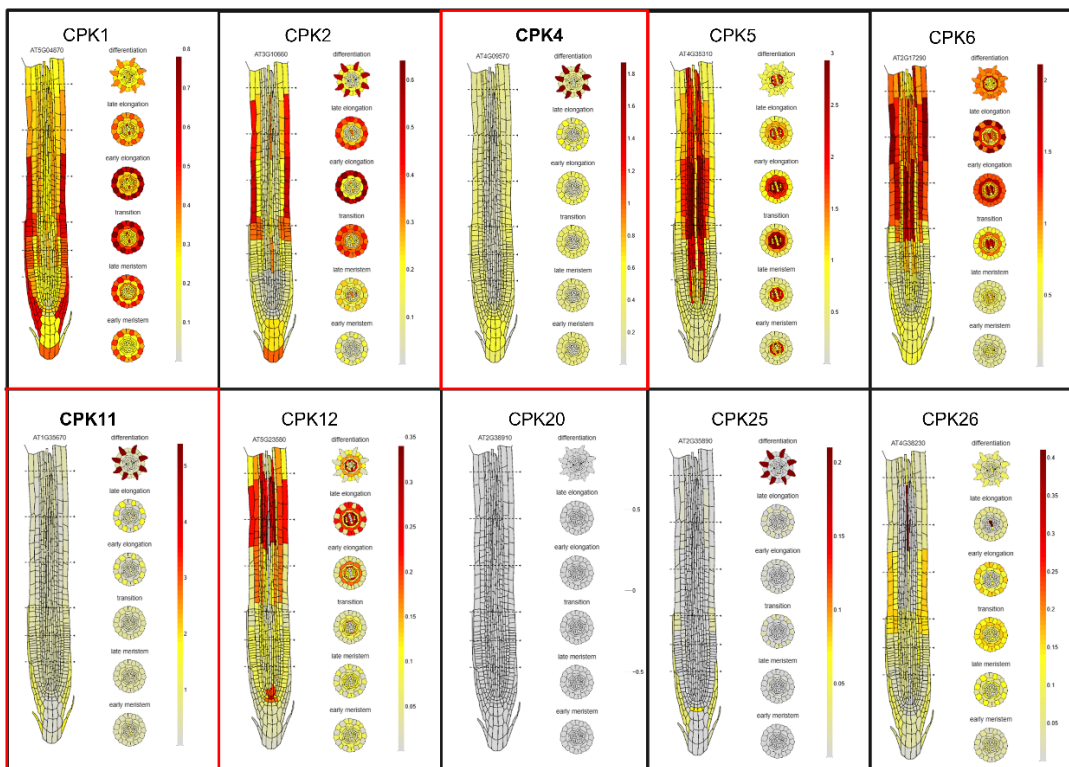


Figure 12. Expression Pattern of CPK Subgroup 1 Members in Arabidopsis Root. This figure, derived from RootCellAtlas data, illustrates the expression patterns of CPK subgroup 1 members across various developmental stages of the Arabidopsis root. CPK4 and CPK11 are specifically emphasized within red boxes, indicating their potential expression in root development and stress response.

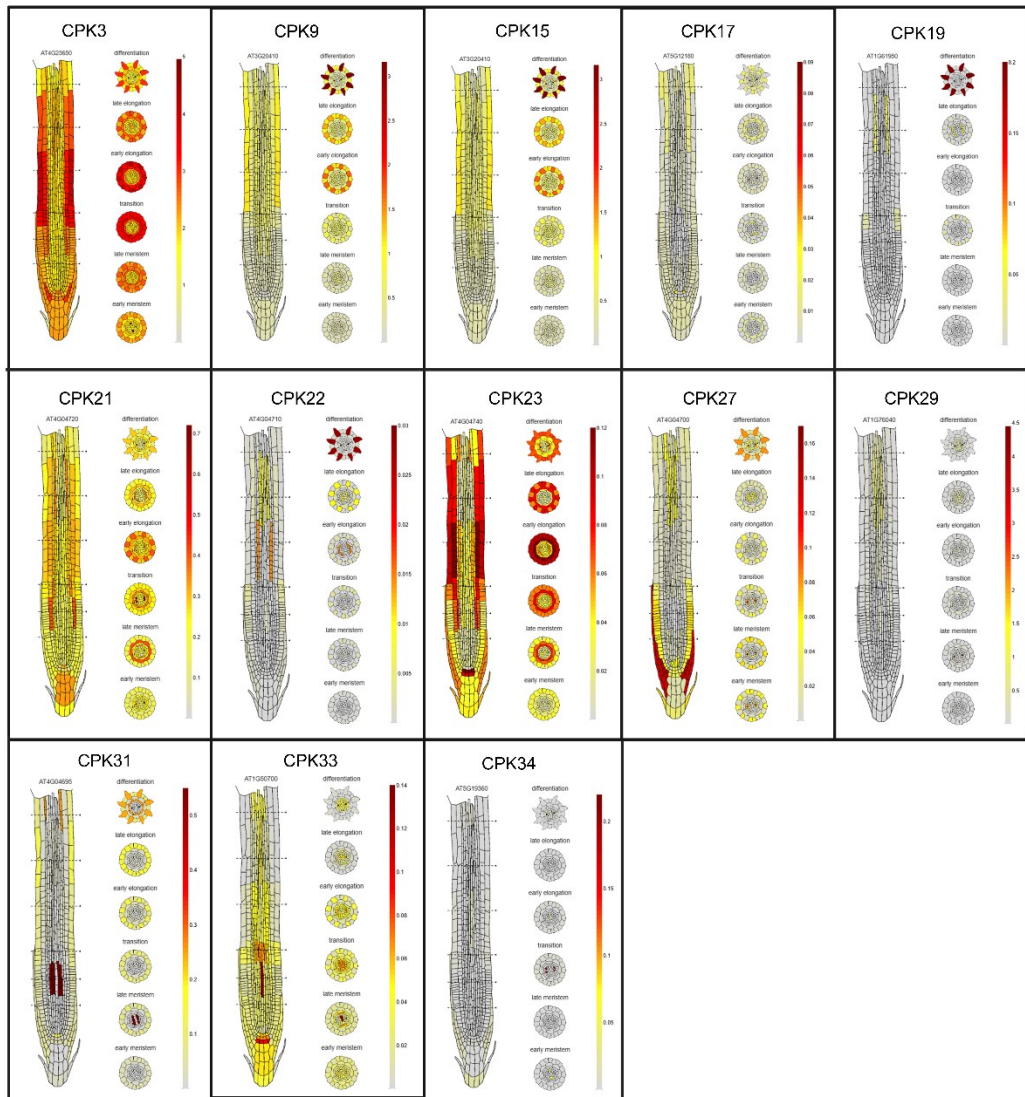


Figure 13. Expression Pattern of CPK Subgroup 2 Members in Arabidopsis Root. This figure, derived from RootCellAtlas data, illustrates the expression patterns of CPK subgroup 2 members across various developmental stages of the Arabidopsis root.

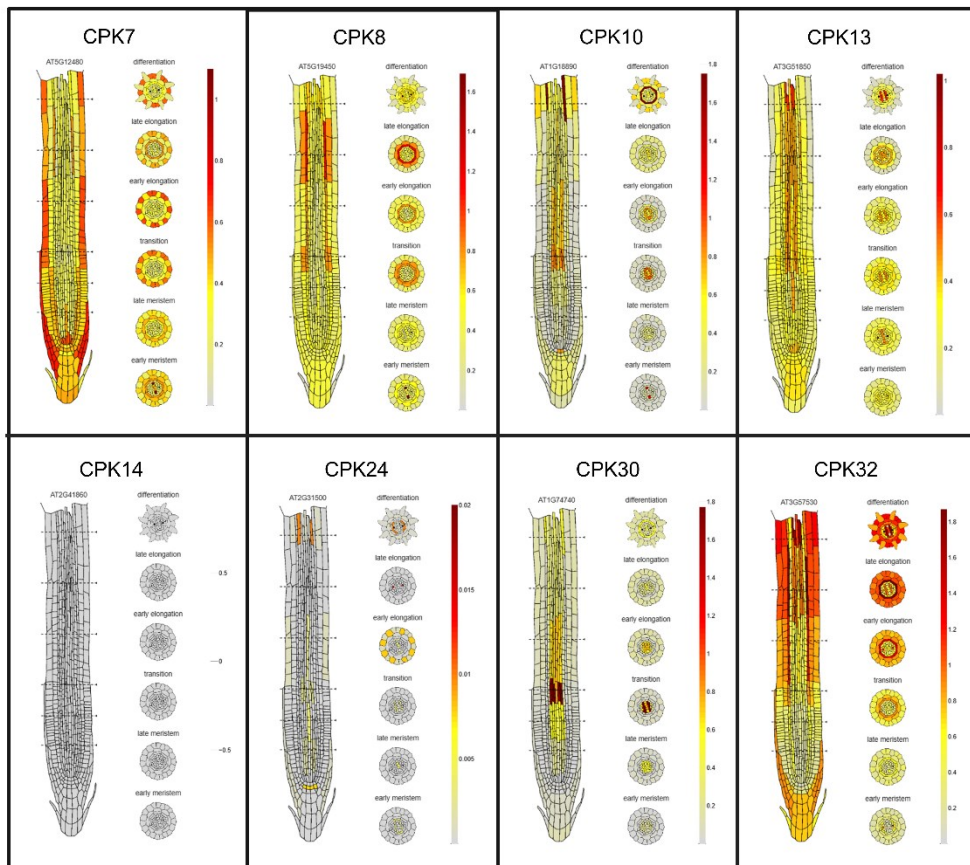


Figure 14. Expression Pattern of CPK Subgroup 3 Members in Arabidopsis Root. This figure, derived from RootCellAtlas data, illustrates the expression patterns of CPK subgroup 3 members across various developmental stages of the Arabidopsis root.

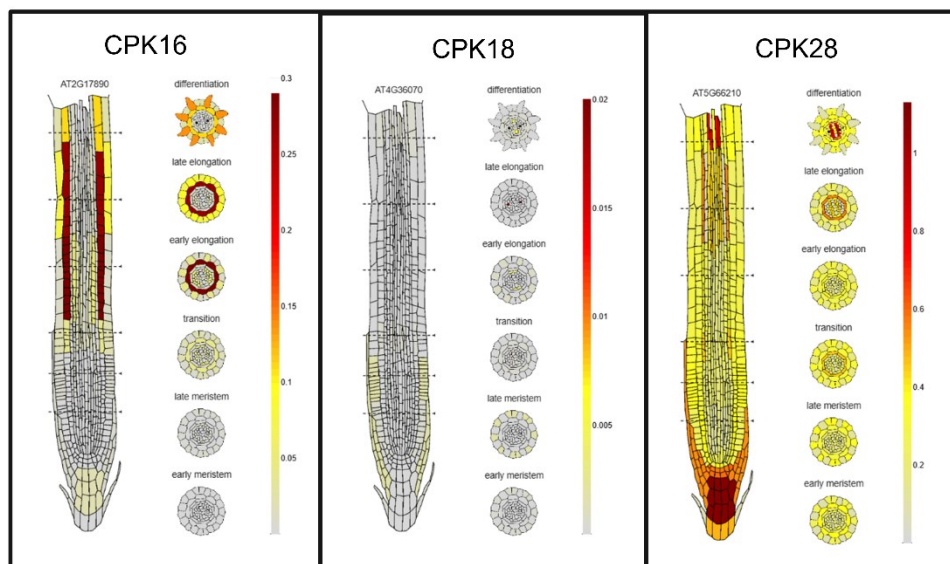


Figure 15. Expression Pattern of CPK Subgroup 4 Members in Arabidopsis Root. This figure, derived from RootCellAtlas data, illustrates the expression patterns of CPK subgroup 4 members across various developmental stages of the Arabidopsis root.

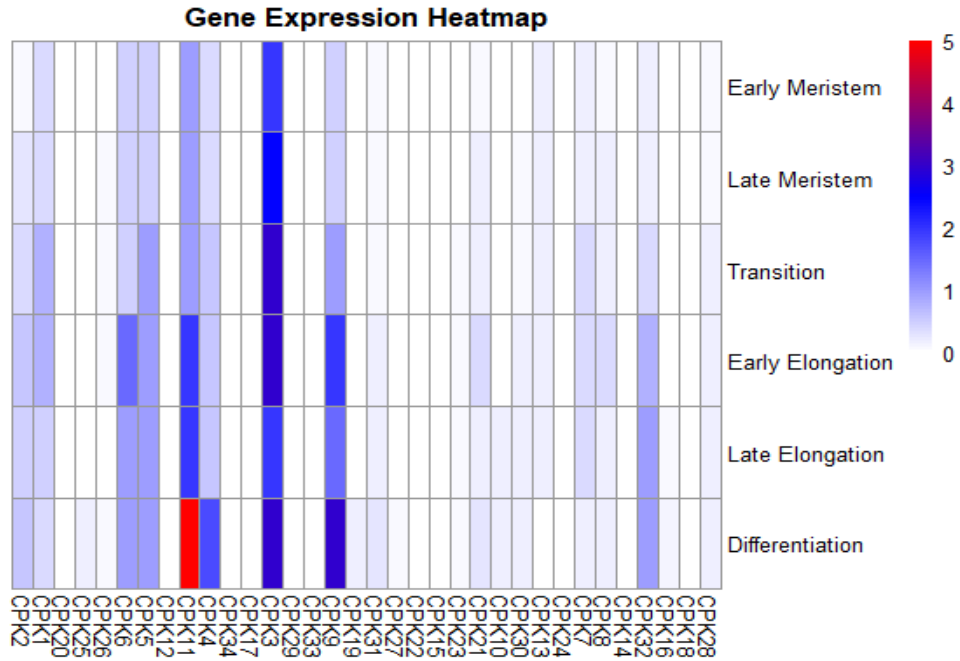


Figure 16. Heatmap of CPK Family Expression Across Root Developmental Stages. This heatmap, generated using the pheatmap package in R (version 4.3.1) from RootCellAtlas data, displays the expression patterns of all CPK family members across various root development.

4.4 Cross-Species Transcriptomic Analysis of Soil Compaction Response in Rice

4.4.1 Identification of Differentially Expressed Genes

When we dove into the RNA-seq data from rice roots grown in compacted versus normal soil, as shared by Zhu et al. (2025), we uncovered a fascinating reshuffling of gene activity triggered by the pressure of compacted earth. To make sure we were looking at the most relevant players, we zeroed in on the outer root layers—the exodermis, sclerenchyma, cortex, and atrichoblast—since these seem to be the first to feel and react to soil stress. We then sifted through the genes, picking out those tied to stress responses, biotic cues, kinase functions, and mechanical pressures, which led us to 112 genes stepping up their game and 50 dialing back. Using the Rice Genome Annotation Project, we traced these rice genes to their Arabidopsis cousins, opening a

window into how these species might share similar tricks.

Two stars stood out among the upregulated genes: CPK4 and CPK11, both calcium-dependent protein kinases. They showed a gentle but meaningful boost, with Log₂ fold change values of 1.02 (p-value = 0.00364) each, linked to Arabidopsis homologs AT4G09570 (CPK4) and AT1G35670 (CPK11). This nudge in activity hints that these genes might help rice roots sense and handle the squeeze of compacted soil. To get a clearer picture, we turned to the ePlant platform to map out how their Arabidopsis relatives behave. We noticed some neat patterns: peroxidases like AT5G15180, which ramped up, huddled together, while expansins like AT5G42510, which toned down, formed their own group—suggesting these stress pathways are a shared heritage. Plus, receptor-like kinases such as AT3G50980 and AT2G18980 cozied up in a kinase network, pointing to a team effort in signaling the mechanical challenge. (Figure 17).

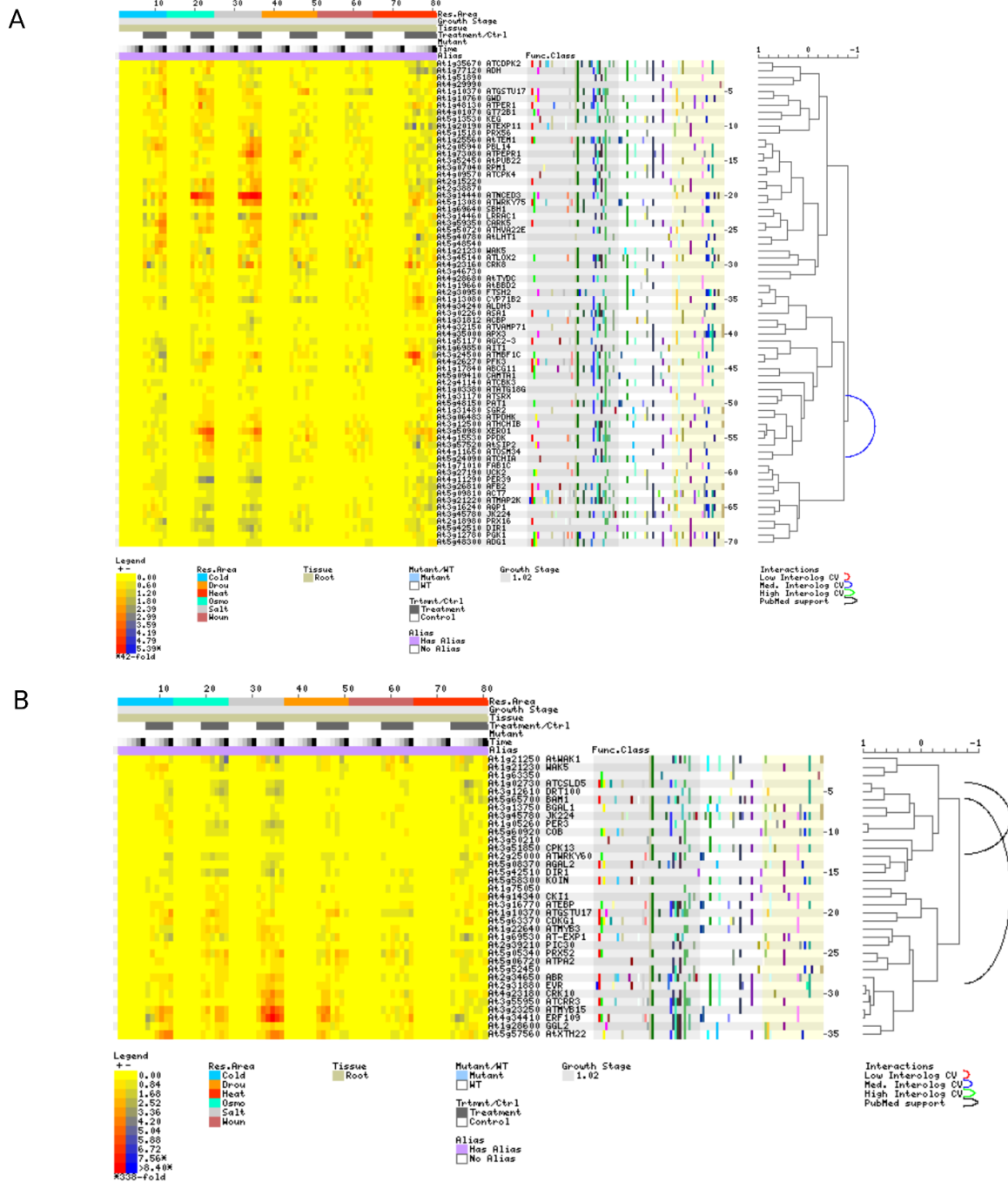


Figure 17. Heatmap Visualization of Gene Expression in Rice Root Tissues. (A) Heatmap of 112 upregulated genes across outer root tissues (exodermis, sclerenchyma, cortex, atrichoblast) under compacted soil conditions, generated using the eFP Browser, highlighting significant transcriptional responses. (B) Heatmap of 50 downregulated genes in the same tissues, also derived from ePlant, illustrating contrasting expression patterns. (Zhu et al., 2025)

4.5 QTL Mapping Suggests Co-Regulation of Mechanosensitive Genes

Our QTL mapping analysis using AraQTL revealed distinct regulatory patterns for *CPK4* and *CPK11*. While *CPK4* showed no significant QTL peaks—hinting at complex, dispersed genetic control or environmental modulation, *CPK11* displayed a robust eQTL signal on Chromosome 1. Intriguingly, this peak coincided with the *ANNEXIN1* locus (Figure 18), raising the possibility of coregulation or functional synergy between these genes in mechanosensitive signaling. The stark contrast in their genetic architectures suggests divergent evolutionary constraints or context-dependent expression mechanisms warranting further investigation.

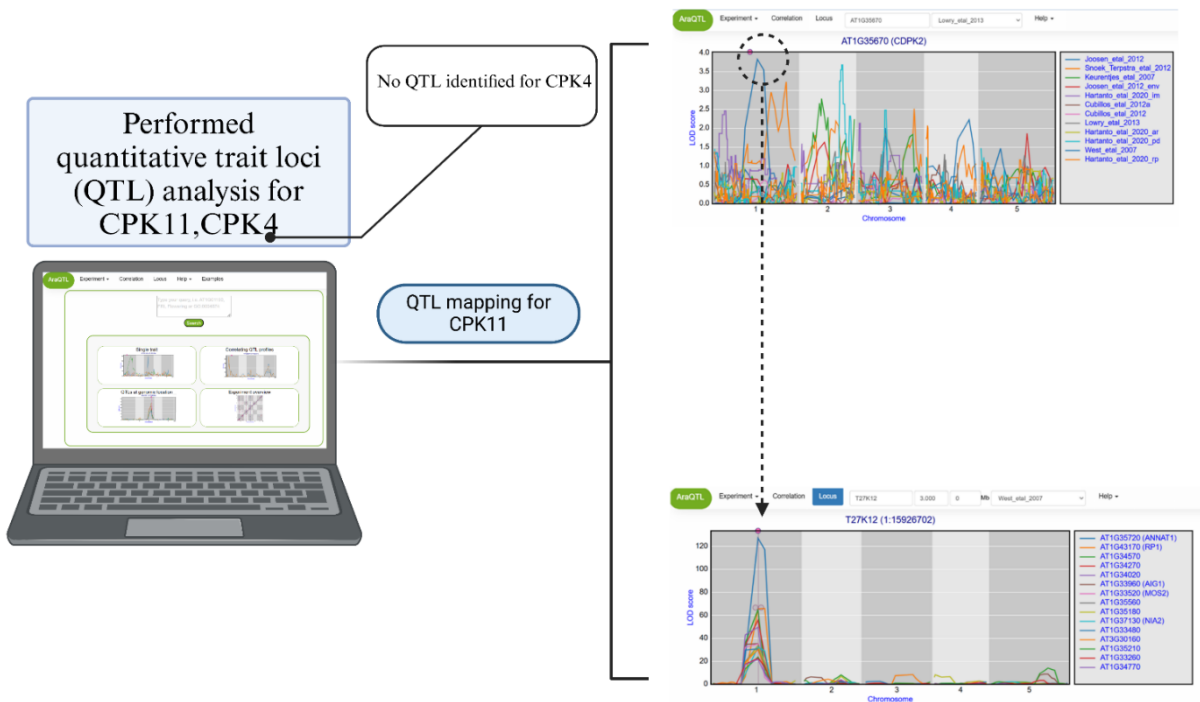


Figure 18. QTL Mapping of CPK4 and CPK11 Expression in Arabidopsis.

4.6 Confirmation of T-DNA Insertion Mutants

PCR genotyping confirmed the homozygosity of all three T-DNA insertion lines—*CPK4* (SALK_081860C), *CPK11* (SALK_054495C), and *ANNEXIN1* (SALK_132169C), using

gene-specific and T-DNA border primers. Amplification patterns were consistent with expected mutant genotypes and no wild-type alleles were detected (Figure 19).

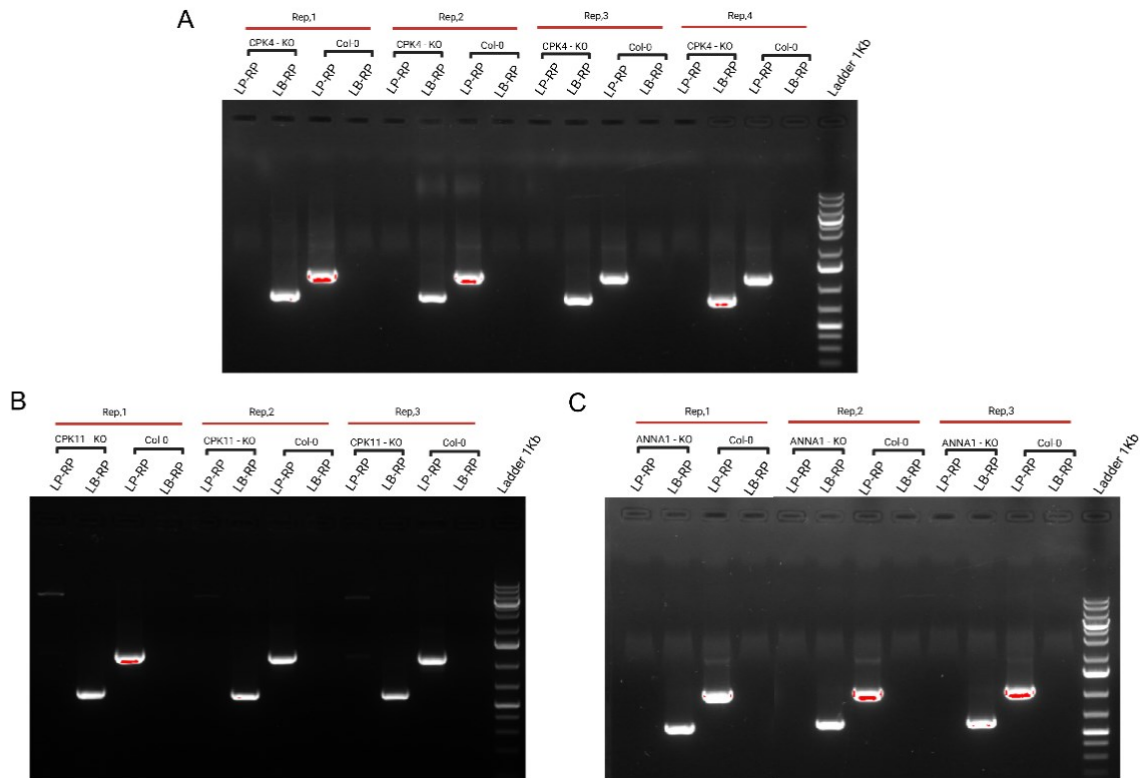


Figure 19. Representative gel images showing genotyping results. A: CPK4 KO, B: CPK11 KO and C: ANNEXIN1 KO

4.7 Root Hair Phenotyping Under Compacted Agar Conditions

Root hair elongation was assessed in wild-type (Col-0) and mutant lines (CPK4 KO, CPK11 KO, ANNEXIN1 KO) under escalating stress conditions (Figure 20).

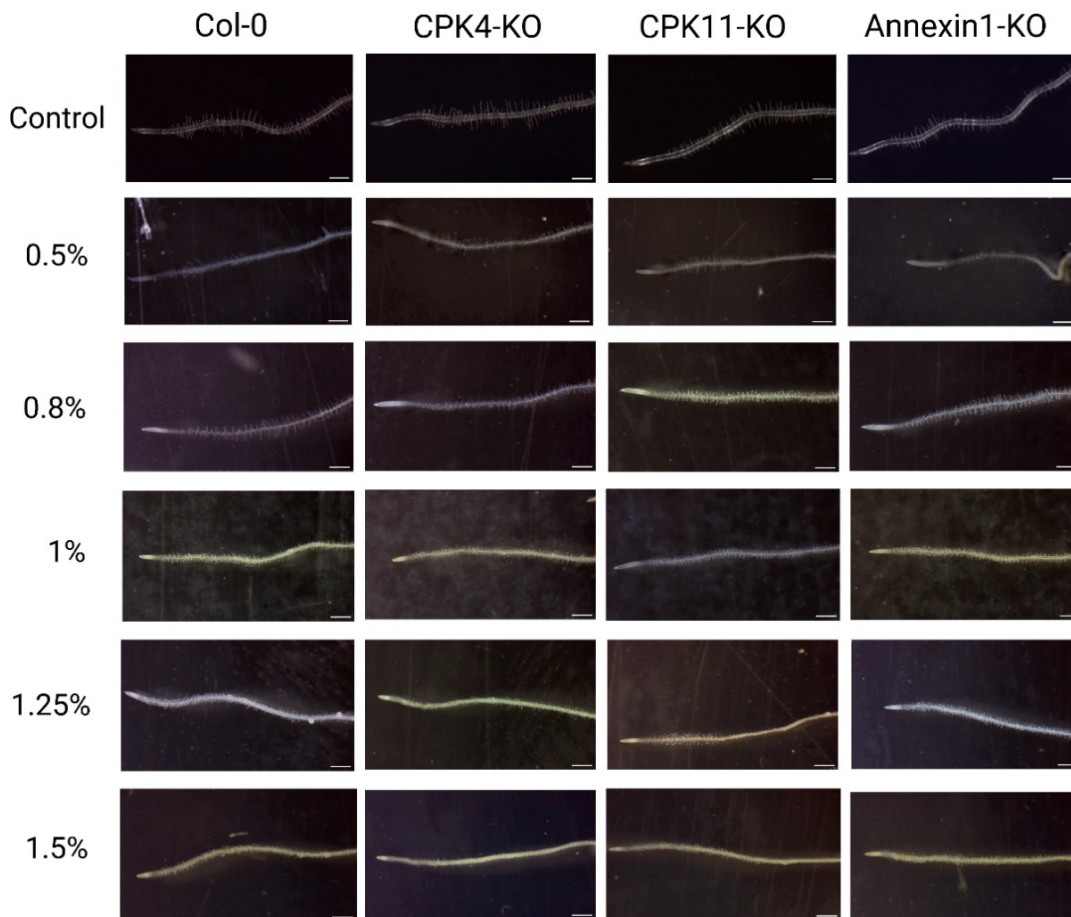


Figure 20. Root Hair Phenotyping Under Compacted Agar Conditions. This figure displays root hair morphology in Col-0 and mutant lines (CPK4 KO, CPK11 KO, ANNEXIN1 KO) under stressed (Concentrated agar) and control condition, with a scale bars = 500 μ m.

4.7.1 Stress-Induced Changes in Root Hair Growth

In Col-0, root hair length decreased steadily with increasing stress, declining from approximately 83% of the control at 0.5% stress to just 19% at the highest concentration (1.5%). This demonstrates a clear negative correlation between stress intensity and root hair growth in the wild type.

The CPK4 knockout mutant exhibited heightened vulnerability to stress at lower concentrations, with root hair growth significantly impaired compared to Col-0. However, under severe stress, CPK4 KO root hair length approached that of the wild type, indicating that CPK4's role may be most critical during early stress exposure.

Interestingly, CPK11-deficient plants displayed an unusual response: root hair elongation was initially higher than Col-0 at 0.5% stress (~90% of control), suggesting a degree of stress

tolerance. However, this advantage disappeared at higher stress levels, with growth inhibition becoming more pronounced than in the wild type. This implies that CPK11 contributes to stress adaptation in a concentration-dependent manner.

The ANNEXIN1 knockout line was the most severely affected, with root hair growth dropping to 48% of control levels at 0.5% stress and nearly ceasing at 1.25% stress. This extreme phenotype highlights ANNEXIN1's essential function in sustaining root hair development under adverse conditions (Graph 21A).

4.7.2 Mutant Sensitivity Relative to Wild-Type

Statistical evaluation (two-way ANOVA with Tukey's post-hoc test) confirmed distinct stress responses among genotypes:

CPK4 KO was significantly more impaired than Col-0 at low-to-moderate stress ($p < 0.0001$), though differences lessened at extreme concentrations.

CPK11 KO showed a unique pattern—enhanced growth at 0.5% stress ($p = 0.0092$) but severe inhibition at higher levels ($p < 0.0001$).

ANNEXIN1 KO was consistently the most vulnerable, with drastic growth reduction at all stress levels ($p < 0.0001$).

These observations suggest that CPK4 and ANNEXIN1 are vital for general stress resilience, while CPK11 may modulate responses in a stress-level-dependent fashion (Graph 21B).

4.7.3 Root Hair Length Analysis (0.8% Stress)

The comparison between surface-grown (control) and medium-embedded (0.8% treatment) seedlings revealed distinct responses among genotypes. While Col-0 wild-type plants showed no significant length difference between control and treated conditions ($p=0.0957$), all mutant lines exhibited marked alterations when treated. CPK4 KO and ANNEXIN1 KO mutants displayed significantly reduced root hair lengths in the treatment group compared to their controls ($p=0.0026$ and $p=0.0016$ respectively). Notably, CPK11 KO showed the most dramatic response, with treated plants differing significantly from both their control ($p=0.0006$) and other genotypes, suggesting a unique sensitivity to growth medium conditions (Graph 21C).

4.7.4 Root Hair Density Analysis

Root hair count analysis demonstrated stress-dependent variations across genotypes. Col-0 maintained stable hair density up to 1% stress, with significant reduction only at 1.5% concentration ($p=0.0009$). In contrast, CPK4 KO mutants showed early and progressive density decreases, becoming significant at 0.5% stress ($p=0.0021$) and most severe at 1.5% ($p<0.0001$). CPK11 KO displayed intermediate sensitivity, with significant reduction only at maximum stress ($p=0.0219$). ANNEXIN1 KO exhibited the most pronounced response, showing complete growth inhibition at higher concentrations, mirroring its length phenotype (Graph 21D).

4.7.5 First Root Hair Emergence Pattern

The distance from root tip to first root hair emergence showed genotype-specific stress responses. Col-0 displayed significant proximal shifting at 0.5% stress ($p=0.0084$) but adapted at higher concentrations. CPK4 KO mutants showed consistent stress sensitivity, with significant proximal shifting at 0.8% ($p=0.0363$). ANNEXIN1 KO exhibited extreme sensitivity at 0.5% stress ($p<0.0001$), while CPK11 KO showed no significant changes, indicating preserved developmental timing despite other stress responses (Graph 21E). critical stage, we focused our study on these two genes to understand their role in hair growth and environmental adaptation.

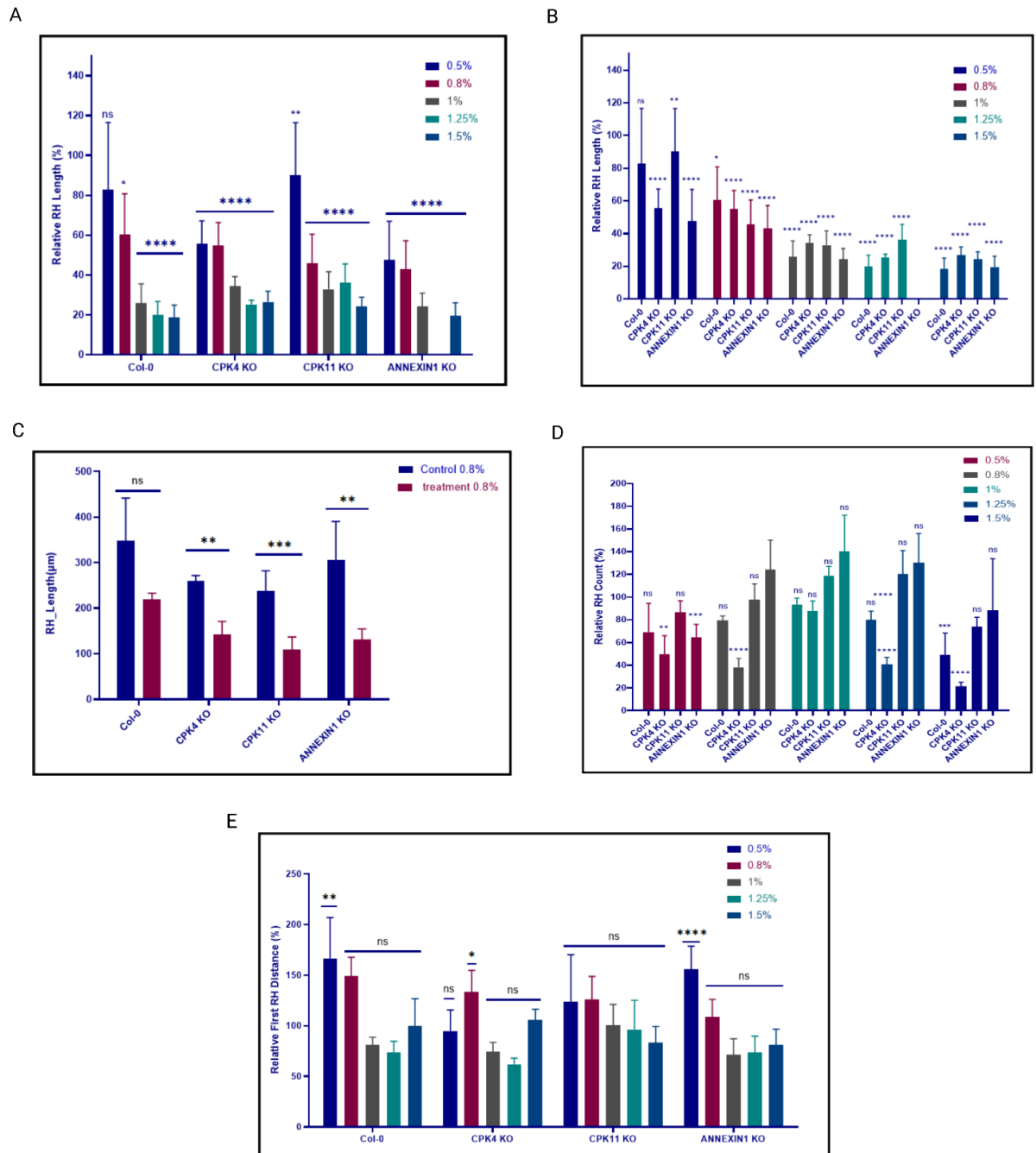


Figure 21. Phenotypic Responses of Root Hairs to Mechanical Stress. (A) Root Hair Length. (B) Mutant Sensitivity Relative to Wild-Type. (C) Root Hair Length Analysis (0.8% Stress). (D) Root Hair Density Analysis. (E) First Root Hair Emergence Pattern.

4.8 RT-PCR and RT-qPCR

Our quantitative PCR (qPCR) analysis investigated the expression dynamics of CPK4, CPK11, and ANNEXIN1 in wild-type (Col-0) and mutant lines (CPK4 KO, CPK11 KO, ANNEXIN1 KO) of *Arabidopsis thaliana* under escalating mechanical stress induced by agar concentrations ranging from 0.5% to 1.5%. Expression levels, normalized to the housekeeping gene ACT8 and compared to unstressed conditions within each genotype, were visualized in Log₂ fold change (Log₂FC) graphs, revealing distinct regulatory patterns (Figure 22). These patterns provide insights into the genes' roles in mechanosensory signaling and their sensitivity to soil compaction-like stress.

In Col-0, CPK4 expression exhibited a biphasic response: a modest downregulation at 0.5% agar (Log₂FC = -0.53) transitioned to a slight increase at 0.8% (Log₂FC = -0.57), followed by a more pronounced downregulation at 1% (Log₂FC = -1.42) and 1.25% (Log₂FC = -0.52), stabilizing with a minor decrease at 1.5% (Log₂FC = -0.33). This suggests an initial adaptive suppression followed by a stress-dependent decline, indicative of a stabilizing role under moderate mechanical stress. CPK11 in Col-0 showed a progressive downregulation with increasing agar concentration, from a minimal change at 0.5% (Log₂FC = -0.47) to significant suppression at 1% (Log₂FC = -2.77) and 1.5% (Log₂FC = -2.08), reflecting its role as a stress intensity sensor. ANNEXIN1 displayed an opposite trend, with slight downregulation at 0.5% (Log₂FC = -0.42) and 0.8% (Log₂FC = -0.89), followed by upregulation at 1% (Log₂FC = 0.19) and a dramatic increase at 1.5% (Log₂FC = 5.99), highlighting its activation under severe mechanical stress.

In the CPK4 KO line, CPK11 expression was markedly upregulated at 0.8% (Log₂FC = 3.12) and 1% (Log₂FC = 1.88), with a reduced increase at 1.5% (Log₂FC = 1.03), suggesting compensatory activation in the absence of CPK4. ANNEXIN1 also showed significant upregulation at 0.8% (Log₂FC = 2.59) and 1% (Log₂FC = 0.65), peaking at 1.25% (Log₂FC = 1.02) and 1.5% (Log₂FC = 3.36), indicating enhanced responsiveness to mechanical stress. As agar concentration increased from 0.5% to 1.5%, CPK4 KO mutants exhibited heightened sensitivity, with ANNEXIN1 showing the most pronounced changes, particularly at higher concentrations.

In the CPK11 KO line, CPK4 expression was downregulated at 0.5% (Log₂FC = -1.34) but showed extreme suppression at 0.8% (Log₂FC = -4.02) and 1% (Log₂FC = -7.67), with a partial

recovery at 1.25% (Log2FC = 1.52) and 1.5% (Log2FC = -1.53). ANNEXIN1 was dramatically upregulated at 0.5% (Log2FC = 3.33) and remained elevated at 0.8% (Log2FC = 2.03), 1% (Log2FC = -0.38), and 1.25% (Log2FC = 4.14), with an extreme peak at 1.5% (Log2FC = 8.60), reflecting a strong compensatory response. This line showed the greatest sensitivity to increasing mechanical stress, with ANNEXIN1 expression changes being the most dynamic compared to Col-0.

In the ANNEXIN1 KO line, CPK4 expression was slightly downregulated at 0.5% (Log2FC = -3.31) but increased at 1% (Log2FC = 1.04) and 1.25% (Log2FC = 1.15), with a minor decrease at 1.5% (Log2FC = 0.84). CPK11 showed downregulation at 0.5% (Log2FC = -3.80) and slight changes at higher concentrations (e.g., 1% Log2FC = 0.62, 1.5% Log2FC = -1.66), indicating reduced stability without ANNEXIN1. This mutant displayed moderate sensitivity, with CPK4 showing the most variable response as stress intensified.

Effects of Increasing Agar Concentration (0.5% to 1.5%): As mechanical stress increased, Col-0 maintained relatively stable CPK4 and ANNEXIN1 expression with a clear CPK11 decline, reflecting a balanced response. CPK4 KO showed escalating ANNEXIN1 and CPK11 upregulation, suggesting compensatory mechanisms. CPK11 KO exhibited the most dramatic shifts, with ANNEXIN1 surging and CPK4 plummeting then recovering, indicating high sensitivity. ANNEXIN1 KO showed variable CPK4 and CPK11 responses, with less pronounced changes, suggesting partial resilience.

Expression Changes and Sensitivity: ANNEXIN1 expression was the most altered across genotypes, with the largest Log2FC range (e.g., 5.99 in Col-0 at 1.5%, 8.60 in CPK11 KO at 1.5%), indicating its heightened sensitivity to mechanical stress. CPK11 KO mutants were the most sensitive overall, with ANNEXIN1 and CPK4 showing the greatest dynamic range compared to Col-0, underscoring their vulnerability to escalating stress. This sensitivity aligns with ANNEXIN1's role as a stress integrator and CPK11's gating function, as visualized in the Log2FC trends (Figure 22).

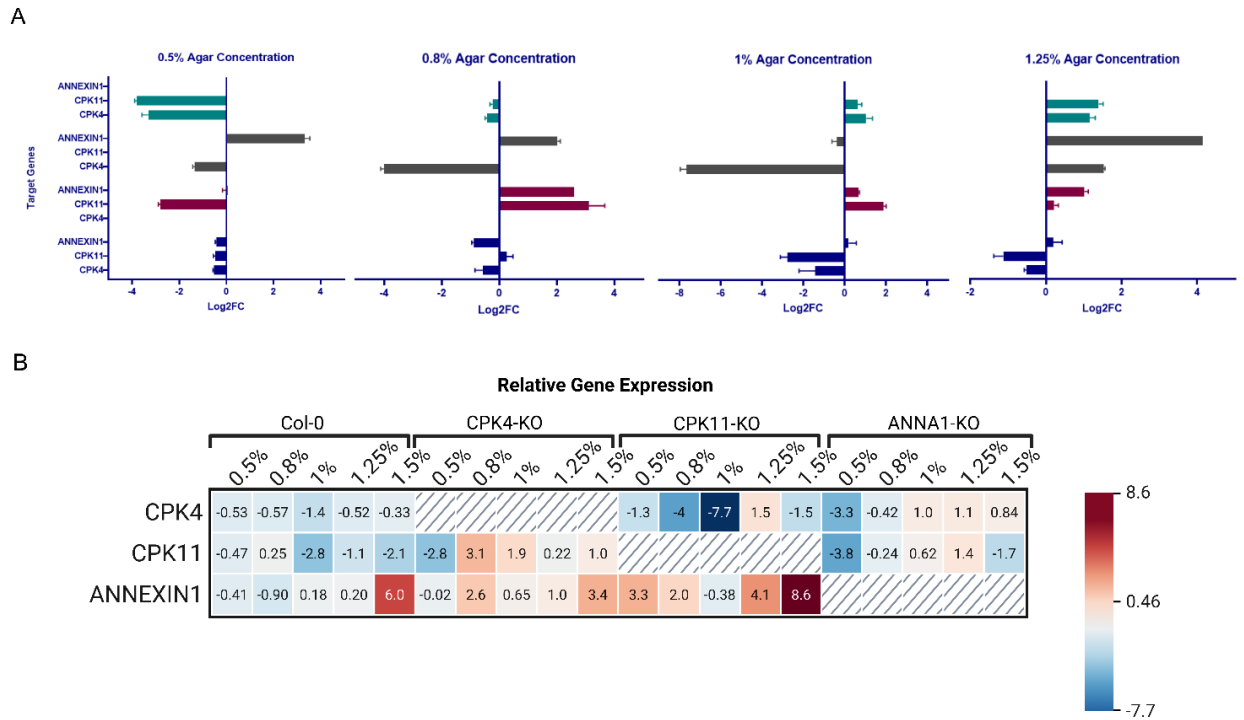


Figure 22. Visualization of qPCR Results for Mechanosensory Genes Under Mechanical Stress. (A) Graphs generated using Prism software depict Log₂ fold change (Log₂FC) expression levels of CPK4, CPK11, and ANNEXIN1 in wild-type (Col-0) and mutant lines (CPK4 KO, CPK11 KO, ANNEXIN1 KO) across agar concentrations (0.5% to 1.5%). (B) A heatmap created with BioRender illustrates the relative expression patterns of these genes.

5 Conclusion

This master's thesis has significantly advanced our understanding of how plant root hairs sense and adapt to mechanical stress, a crucial process for plant survival in challenging soil environments. A foundational achievement of this work was the successful development and validation of two novel root hair isolation techniques: cryo-mechanical disruption and freeze-thaw lysis. These methods proved highly effective, enabling specific and contamination-free sampling for detailed molecular analyses, as confirmed by microscopy, RNA integrity tests, and the enrichment or depletion of specific marker genes like EXP7/RSL4 and SCR/SHR.

Through extensive phenotyping experiments under varying levels of agar-induced mechanical stress (ranging from 0.5% to 1.5% agar), we uncovered the distinct and often compensatory roles of CPK4, CPK11, and ANNEXIN1. Our findings indicate that CPK4 is essential for the plant's early resilience to stress, with *cpk4* mutants showing hypersensitivity even at mild ($\leq 1\%$)

agar concentrations. CPK11, on the other hand, appears to act as a sophisticated "tuner" for stress intensity; it surprisingly enhanced root hair growth at mild stress (0.5% agar) but severely impaired it at higher concentrations. Most strikingly, ANNEXIN1 emerged as a critical fail-safe mechanism, with annexin1 mutants exhibiting near-complete growth arrest when faced with severe stress ($\geq 1.25\%$ agar).

Further investigation using quantitative PCR (qPCR) revealed a fascinating hierarchical crosstalk at the transcriptional level. The loss of CPK4 triggered a significant upregulation of CPK11 (Log₂FC 3.12 at 0.8% agar) and a notable induction of ANNEXIN1 (Log₂FC 3.36 at 1.5% agar). Even more dramatically, the absence of CPK11 led to a hyper-induction of ANNEXIN1 (Log₂FC 8.60 at 1.5% agar), strongly suggesting that ANNEXIN1 plays a crucial compensatory role when these kinases are compromised. The broader significance of these findings is underscored by their evolutionary conservation; we observed that rice homologs of CPK4 and CPK11 were similarly upregulated in compacted soil (Log₂FC 1.02, $p = 0.00364$), confirming their conserved roles in mechanosensing across different plant species. Intriguingly, QTL mapping also revealed that ANNEXIN1 co-localizes with CPK11 on Chromosome 1, hinting at a potential co-regulation or direct interaction.

Based on these insights, we propose a refined model for root hair mechanosensing: CPK4 appears to stabilize the initial stress responses, CPK11 modulates adaptation to varying pressure intensities, and ANNEXIN1 integrates signals under severe stress, effectively acting as the "final defender" of root hair integrity. Beyond this conceptual model, our newly developed isolation methods provide a valuable toolkit, empowering future cell-specific studies in root hair mechanobiology. The observed conservation of this pathway in rice holds significant implications, suggesting that targeting these genes could offer a promising avenue for enhancing root penetration and overall crop resilience in compacted soils.

While this research provides a robust foundation, it's important to acknowledge certain limitations. Our use of agar plates, while providing controlled conditions, simplifies the inherent complexity and heterogeneity of natural soil environments, meaning responses might differ in real-world settings. Furthermore, our functional testing was limited to only three genes, even though CPKs and annexins operate within much broader, interconnected signaling networks. Lastly, the interactions between CPK4/CPK11 and ANNEXIN1 were primarily inferred from indirect evidence; future studies employing techniques like co-immunoprecipitation or FRET would be crucial to validate any direct physical binding at the

protein level. Looking ahead, several exciting avenues for future work emerge. It would be highly beneficial to test our mutants in more realistic compacted soils or specialized microfluidic devices that can accurately simulate soil pores. Live-tracking spatiotemporal calcium (Ca²⁺) dynamics in root hairs of mutants under stress using advanced imaging techniques would provide invaluable real-time insights. Expanding the genetic network by profiling other CDPKs (e.g., CPK5, CPK6) and annexins known to be linked to mechanosensing could reveal a more complete picture. Ultimately, translating these findings to agriculturally relevant crops by engineering CPK11 and ANNEXIN1 orthologs in species like rice or wheat would be essential to validate their field-level benefits for sustainable agriculture.

References

Colombi T, Torres LC, Walter A, Keller T. Feedbacks between soil penetration resistance, root architecture and water uptake limit water accessibility and crop growth—A vicious circle. *Science of the Total Environment*. 2018 Jun 1;626:1026-35.

Bowles AM, Paps J, Bechtold U. Water-related innovations in land plants evolved by different patterns of gene cooption and novelty. *New Phytologist*. 2022 Jul;235(2):732-42.

Zhu X, Peng W, Xie Q, Ran E. Effects of soil compaction stress combined with drought on soil pore structure, root system development, and maize growth in early stage. *Plants*. 2024 Nov 13;13(22):3185.

Vasseur F, Exposito-Alonso M, Ayala-Garay OJ, Wang G, Enquist BJ, Vile D, Violle C, Weigel D. Adaptive diversification of growth allometry in the plant *Arabidopsis thaliana*. *Proceedings of the National Academy of Sciences*. 2018 Mar 27;115(13):3416-21.

Zandalinas SI, Fritschi FB, Mittler R. Global warming, climate change, and environmental pollution: recipe for a multifactorial stress combination disaster. *Trends in Plant Science*. 2021 Jun 1;26(6):588-99.

Dodds PN, Rathjen JP. Plant immunity: towards an integrated view of plant–pathogen

interactions. *Nature Reviews Genetics*. 2010 Aug;11(8):539-48.

Millet YA, Danna CH, Clay NK, Songnuan W, Simon MD, Werck-Reichhart D, Ausubel FM. Innate immune responses activated in *Arabidopsis* roots by microbe-associated molecular patterns. *The Plant Cell*. 2010 Mar 1;22(3):973-90.

Chen T, Nomura K, Wang X, Sohrabi R, Xu J, Yao L, Paasch BC, Ma LI, Kremer J, Cheng Y, Zhang L. A plant genetic network for preventing dysbiosis in the phyllosphere. *Nature*. 2020 Apr 30;580(7805):653-7.

Dinneny JR. Developmental responses to water and salinity in root systems. *Annual Review of Cell and Developmental Biology*. 2019 Oct 6;35(1):239-57.

Fendrych M, Akhmanova M, Merrin J, Glanc M, Hagihara S, Takahashi K, Uchida N, Torii KU, Friml J. Rapid and reversible root growth inhibition by TIR1 auxin signalling. *Nature plants*. 2018 Jul;4(7):453-9.

Kochian LV, Piñeros MA, Liu J, Magalhaes JV. Plant adaptation to acid soils: the molecular basis for crop aluminum resistance. *Annual review of plant biology*. 2015 Apr 29;66(1):571-98.

Riaz M, Kamran M, Fang Y, Wang Q, Cao H, Yang G, Deng L, Wang Y, Zhou Y, Anastopoulos I, Wang X. Arbuscular mycorrhizal fungi-induced mitigation of heavy metal phytotoxicity in metal contaminated soils: A critical review. *Journal of Hazardous Materials*. 2021 Jan 15;402:123919.

DalCorso G, Fasani E, Manara A, Visioli G, Furini A. Heavy metal pollutions: state of the art and innovation in phytoremediation. *International journal of molecular sciences*. 2019 Jul 11;20(14):3412.

Hamilton ES, Schlegel AM, Haswell ES. United in diversity: mechanosensitive ion channels in plants. *Annual review of plant biology*. 2015 Apr 29;66(1):113-37.

Nakagawa Y, Katagiri T, Shinozaki K, Qi Z, Tatsumi H, Furuichi T, Kishigami A, Sokabe M, Kojima I, Sato S, Kato T. *Arabidopsis* plasma membrane protein crucial for Ca²⁺ influx

and touch sensing in roots.

Proceedings of the National Academy of Sciences. 2007 Feb 27;104(9):3639-44.

Pomiès L, Decourteix M, Franchel J, Moulia B, Leblanc-Fournier N. Poplar stem transcriptome is massively remodelled in response to single or repeated mechanical stimuli. *Bmc Genomics*. 2017 Dec;18:1-6.

Xu W, Purugganan MM, Polisensky DH, Antosiewicz DM, Fry SC, Braam J. Arabidopsis TCH4, regulated by hormones and the environment, encodes a xyloglucan endotransglycosylase. *The Plant Cell*. 1995 Oct 1;7(10):1555-67.

Zheng Z, Guo Y, Novák O, Chen W, Ljung K, Noel JP, Chory J. Local auxin metabolism regulates environment-induced hypocotyl elongation. *Nature plants*. 2016 Mar 21;2(4):1-9.

Bengough AG, McKenzie BM, Hallett PD, Valentine TA. Root elongation, water stress, and mechanical impedance: a review of limiting stresses and beneficial root tip traits. *Journal of experimental botany*. 2011 Jan 1;62(1):59-68.

Helliwell JR, Sturrock CJ, Mairhofer S, Craigon J, Ashton RW, Miller AJ, Whalley WR, Mooney SJ. The emergent rhizosphere: imaging the development of the porous architecture at the root-soil interface. *Scientific reports*. 2017 Nov 1;7(1):14875.

Huang G, Kilic A, Karady M, Zhang J, Mehra P, Song X, Sturrock CJ, Zhu W, Qin H, Hartman S, Schneider HM. Ethylene inhibits rice root elongation in compacted soil via ABA-and auxin-mediated mechanisms. *Proceedings of the National Academy of Sciences*. 2022 Jul 26;119(30):e2201072119.

Jacobsen AG, Jervis G, Xu J, Topping JF, Lindsey K. Root growth responses to mechanical impedance are regulated by a network of ROS, ethylene and auxin signalling in Arabidopsis. *New Phytologist*. 2021 Jul;231(1):225-42.

Nawaz MF, Bourrie G, Trolard F. Soil compaction impact and modelling. A review. *Agronomy for sustainable development*. 2013 Apr;33:291-309.

Tracy SR, Black CR, Roberts JA, Mooney SJ. Soil compaction: a review of past and present techniques for investigating effects on root growth. *Journal of the Science of Food and Agriculture*. 2011 Jul;91(9):1528-37.

Singh Gahoonia T, Nielsen NE. Root traits as tools for creating phosphorus efficient crop varieties. *Plant and Soil*. 2004 Mar;260:47-57.

Baluška F, Salaj J, Mathur J, Braun M, Jasper F, Šamaj J, Chua NH, Barlow PW, Volkmann D. Root hair formation: F-actin-dependent tip growth is initiated by local assembly of profilin-supported F-actin meshworks accumulated within expansin-enriched bulges. *Developmental biology*. 2000 Nov 15;227(2):618-32.

Miller DD, De Ruijter NC, Bisseling T, Emons AM. The role of actin in root hair morphogenesis: studies with lipochito-oligosaccharide as a growth stimulator and cytochalasin as an actin perturbing drug. *The Plant Journal*. 1999 Jan;17(2):141-54.

Park S, Szumlanski AL, Gu F, Guo F, Nielsen E. A role for CSLD3 during cell-wall synthesis in apical plasma membranes of tip-growing root-hair cells. *Nature cell biology*. 2011 Aug;13(8):973-80.

Vissenberg K, Fry SC, Verbelen JP. Root hair initiation is coupled to a highly localized increase of xyloglucan endotransglycosylase action in *Arabidopsis* roots. *Plant Physiology*. 2001 Nov 1;127(3):1125-35.

Marin M, Feeney DS, Brown LK, Naveed M, Ruiz S, Koebernick N, Bengough AG, Hallett PD, Roose T, Puértolas J, Dodd IC. Significance of root hairs for plant performance under contrasting field conditions and water deficit. *Annals of botany*. 2021 Jun 30;128(1):1-6.

Kohli PS, Maurya K, Thakur JK, Bhosale R, Giri J. Significance of root hairs in developing stress-resilient plants for sustainable crop production. *Plant, Cell & Environment*. 2022 Mar;45(3):677-94.

Pereira D, Alline T, Cascaro L, Lin E, Asnacios A. Mechanical resistance of the environment affects root hair growth and nucleus dynamics. *Scientific Reports*. 2024 Jun 14;14(1):13788.

Bacete L, Melida H, Miedes E, Molina A. Plant cell wall-mediated immunity: cell wall changes trigger disease resistance responses. *The Plant Journal*. 2018 Feb;93(4):614-36.

Berardini TZ, Reiser L, Li D, Mezheritsky Y, Muller R, Strait E, Huala E. The Arabidopsis information resource: making and mining the “gold standard” annotated reference plant genome. *genetics*. 2015 Aug;53(8):474-85.

Provart NJ, Alonso J, Assmann SM, Bergmann D, Brady SM, Brkljacic J, Browse J, Chapple C, Colot V, Cutler S, Dangl J. 50 years of Arabidopsis research: highlights and future directions. *New Phytologist*. 2016 Feb;209(3):921-44.

Hamilton ES, Jensen GS, Maksaev G, Katims A, Shero AM, Haswell ES. Mechanosensitive channel MSL8 regulates osmotic forces during pollen hydration and germination. *Science*. 2015 Oct 23;350(6259):438-41.

Fichman Y, Mittler R. Rapid systemic signaling during abiotic and biotic stresses: is the ROS wave master of all trades? . *The Plant Journal*. 2020 Jun;102(5):887-96.

Kudla J, Becker D, Grill E, Hedrich R, Hippler M, Kummer U, Parniske M, Romeis T, Schumacher K. Advances and current challenges in calcium signaling. *New Phytologist*. 2018 Apr;218(2):414-31.

Thor K, Jiang S, Michard E, George J, Scherzer S, Huang S, Dindas J, Derbyshire P, Leitão N, DeFalco TA, Koester P. The calcium-permeable channel OSCA1.3 regulates plant stomatal immunity. *Nature*. 2020 Sep 24;585(7826):569-73.

Tian W, Wang C, Gao Q, Li L, Luan S. Calcium spikes, waves and oscillations in plant development and biotic interactions. *Nature plants*. 2020 Jul;6(7):750-9.

Boudsocq M, Sheen J. CDPKs in immune and stress signaling. *Trends in plant science*. 2013 Jan 1;18(1):30-40.

Ludwig AA, Saitoh H, Felix G, Freyermark G, Miersch O, Wasternack C, Boller T, Jones JD, Romeis T. Ethylene-mediated cross-talk between calcium-dependent protein kinase and MAPK signaling controls stress responses in plants. *Proceedings of the National Academy of Sciences*. 2005 Jul 26;102(30):10736-41.

Simeunovic A, Mair A, Wurzinger B, Teige M. Know where your clients are: subcellular

localization and targets of calcium-dependent protein kinases. *Journal of experimental botany*. 2016 Jun 1;67(13):3855-72.

Bacete L, Melida H, Miedes E, Molina A. Plant cell wall-mediated immunity: cell wall changes trigger disease resistance responses. *The Plant Journal*. 2018 Feb;93(4):614-36.

Yip Delormel T, Boudsocq M. Properties and functions of calcium-dependent protein kinases and their relatives in *Arabidopsis thaliana*. *New Phytologist*. 2019 Oct;224(2):585-604.

Zhu SY, Yu XC, Wang XJ, Zhao R, Li Y, Fan RC, Shang Y, Du SY, Wang XF, Wu FQ, Xu YH. Two calcium-dependent protein kinases, CPK4 and CPK11, regulate abscisic acid signal transduction in *Arabidopsis*. *The Plant Cell*. 2007 Oct 1;19(10):3019-36.

Xu T, Niu J, Jiang Z. Sensing mechanisms: calcium signaling mediated abiotic stress in plants. *Frontiers in plant science*. 2022 Jun 13;13:925863

Krämer U. The natural history of model organisms: Planting molecular functions in an ecological context with *Arabidopsis thaliana*. 2015.

Vissenberg K, Claeijs N, Balcerowicz D, Schoenaers S. Hormonal regulation of root hair growth and responses to the environment in *Arabidopsis*. *Journal of Experimental Botany*. 2020 Apr 23;71(8):2412-27.

Ogorek, Lucas L. Peralta, et al. "Soil compaction sensing mechanisms and root responses." *Trends in Plant Science* (2024).

Zartdinova R, Nikitin A. Calcium in the life cycle of legume root nodules. *Indian Journal of Microbiology*. 2023 Dec;63(4):410-20.

Luan S, Wang C. Calcium signaling mechanisms across kingdoms. *Annual Review of Cell and Developmental Biology*. 2021 Oct 6;37(1):311-40.

Tong T, Li Q, Jiang W, Chen G, Xue D, Deng F, Zeng F, Chen ZH. Molecular evolution of calcium signaling and transport in plant adaptation to abiotic stress. *International Journal of Molecular Sciences*. 2021 Nov 15;22(22):12308.

Dong Q, Wallrad L, Almutairi BO, Kudla J. Ca²⁺ signaling in plant responses to abiotic stresses. *Journal of integrative plant biology*. 2022 Feb;64(2):287-300.

Kang X, Zhao L, Liu X. Calcium signaling and the response to heat shock in crop plants. *International Journal of Molecular Sciences*. 2023 Dec 26;25(1):324.

Negi NP, Prakash G, Narwal P, Panwar R, Kumar D, Chaudhry B, Rustagi A. The calcium connection: exploring the intricacies of calcium signaling in plant-microbe interactions. *Frontiers in Plant Science*. 2023 Oct 2;14:1248648.

Naz M, Afzal MR, Raza MA, Pandey S, Qi S, Dai Z, Du D. Calcium (Ca²⁺) signaling in plants: A plant stress perspective. *South African Journal of Botany*. 2024 Jun 1;169:464-85.

Köster P, DeFalco TA, Zipfel C. Ca²⁺ signals in plant immunity. *The EMBO journal*. 2022 Jun 14;41(12):e110741.

Kilian J, Whitehead D, Horak J, Wanke D, Weini S, Batistic O, D'Angelo C, Bornberg-Bauer E, Kudla J, Harter K. The AtGenExpress global stress expression data set: protocols, evaluation and model data analysis of UV-B light, drought and cold stress responses. *The Plant Journal*. 2007 Apr;50(2):347-63.

Zhu M, Hsu CW, Peralta Ogorek LL, Taylor IW, La Cavera S, Oliveira DM, Verma L, Mehra P, Mijar M, Sadanandom A, Perez-Cota F. Single-cell transcriptomics reveal how root tissues adapt to soil stress. *Nature*. 2025 Apr 30:1-9.

Pereira D, Alline T, Cascaro L, Lin E, Asnacios A. Mechanical resistance of the environment affects root hair growth and nucleus dynamics. *Scientific Reports*. 2024 Jun 14;14(1):13788.

Haling RE, Brown LK, Bengough AG, Young IM, Hallett PD, White PJ, George TS. Root hairs improve root penetration, root-soil contact, and phosphorus acquisition in soils of different

strength. *Journal of experimental botany*. 2013 Sep 1;64(12):3711-21.

Atif RM, Shahid L, Waqas M, Ali B, Rashid MA, Azeem F, Nawaz MA, Wani SH, Chung G. Insights on calcium-dependent protein kinases (CPKs) signaling for abiotic stress tolerance in plants. *International journal of molecular sciences*. 2019 Oct 24;20(21):5298.